This is a repository copy of *Influence of high-latitude blocking and the northern stratospheric polar vortex on cold-air outbreaks under Arctic amplification of global warming*.

White Rose Research Online URL for this paper:
https://eprints.whiterose.ac.uk/221549/

Version: Published Version

**TOPICAL REVIEW • OPEN ACCESS**

# Influence of high-latitude blocking and the northern stratospheric polar vortex on cold-air outbreaks under Arctic amplification of global warming

View the article online for updates and enhancements.

# ENVIRONMENTAL RESEARCH
## CLIMATE

**TOPICAL REVIEW**

# Influence of high-latitude blocking and the northern stratospheric polar vortex on cold-air outbreaks under Arctic amplification of global warming

Edward Hanna[1,*] , Jennifer Francis[2] , Muyin Wang[3] , James E Overland[4] , Judah Cohen[5] , Dehai Luo[6] , Timo Vihma[7] , Qiang Fu[8] , Richard J Hall[9] , Ralf Jaiser[10] , Seong-Joong Kim[11] , Raphael Köhler[10] , Linh Luu[1,15] , Xiaocen Shen[12] , Irene Erner[7] , Jinro Ukita[13] , Yao Yao[6] , Kunhui Ye[14] , Hyesun Choi[11] and Natasa Skific[2]

[1] Department of Geography and Lincoln Climate Research Group, University of Lincoln, Lincoln, United Kingdom
[2] Woodwell Climate Research Center, Falmouth, Massachusetts, United States of America
[3] University of Washington & Pacific Marine Environmental Laboratory (PMEL), Seattle, United States of America
[4] NOAA/PMEL, Seattle, United States of America
[5] Atmospheric & Environmental Research/Massachusetts Institute of Technology, Lexington/Cambridge, MA, United States of America
[6] Key Laboratory of Earth System Numerical Modelling and Application, and CAS Key Laboratory of Regional Climate-Environment for Temperate East Asia, Institute of Atmospheric Physics, Chinese Academy of Sciences, Beijing, People's Republic of China
[7] Finnish Meteorological Institute, Helsinki, Finland
[8] University of Washington, Seattle, United States of America
[9] Department of Physics, Imperial College London, London, United Kingdom
[10] Alfred Wegener Institute, Potsdam, Germany
[11] Korea Polar Research Institute, Incheon, Republic of Korea
[12] Department of Meteorology, University of Reading, Reading, United Kingdom
[13] The University of Tokyo, Kashiwa, Japan
[14] Atmospheric, Oceanic and Planetary Physics, University of Oxford, Oxford, United Kingdom
[15] Vietnam Institute of Meteorology, Hydrology and Climate Change, Hanoi, Vietnam
* Author to whom any correspondence should be addressed.

E-mail: ehanna@lincoln.ac.uk

## Abstract

It is widely accepted that Arctic amplification (AA)—enhanced Arctic warming relative to global warming—will increasingly moderate cold-air outbreaks (CAOs) to the midlatitudes. Yet, some recent studies also argue that AA over the last three decades to the rest of the present century may contribute to more frequent severe winter weather including disruptive cold spells. To prepare society for future extremes, it is necessary to resolve whether AA and severe midlatitude winter weather are coincidental or physically linked. Severe winter weather events in the northern continents are often related to a range of stratospheric polar vortex (SPV) configurations and atmospheric blocking, but these dynamical drivers are complex and still not fully understood. Here we review recent research advances and paradigms including a nonlinear theory of atmospheric blocking that helps to explain the location, timing and duration of AA/midlatitude weather connections, studies of the polar vortex's zonal asymmetric and intra-seasonal variations, its southward migration over continents, and its surface impacts. We highlight novel understanding of SPV variability—polar vortex stretching and a stratosphere–troposphere oscillation—that have remained mostly hidden in the predominant research focus on sudden stratospheric warmings. A physical explanation of the two-way vertical coupling process between the polar vortex and blocking highs, taking into account local surface conditions, remains elusive. We conclude that evidence exists for tropical preconditioning of Arctic-midlatitude climate linkages. Recent research using very large-ensemble climate modelling provides an emerging opportunity to robustly

quantify internal atmospheric variability when studying the potential response of midlatitude CAOs to AA and sea-ice loss.

## 1. Introduction

Accompanied by a rapid loss of Arctic sea-ice in recent decades, the Arctic has warmed four times faster than the global mean annually based on observed data since 1980 (Dai *et al* 2019, Rantanen *et al* 2022, Sweeney *et al* 2023, Zhou *et al* 2024). Despite this Arctic amplification (AA), a surprising number of historic cold-air outbreaks (CAOs) have occurred in the United States (US) and Eurasia in recent years, the frequency of which may even be increasing regionally during the period of AA (Cohen *et al* 2021, 2023, Li *et al* 2022, Ding *et al* 2021, Yao *et al* 2022, 2023). In 2021 and 2022, two of the deadliest and costliest US natural disasters were related to extreme cold events and/or heavy snowfall (NOAA National Centers for Environmental Information (NCEI) 2023), while during January 2024 CAOs with record and near-record low daily temperatures associated with an amplified jet stream configuration and stretched stratospheric polar vortex (SPV) occurred over the central USA and Scandinavia (Barlow 2024, Eichmann 2024). Severe CAOs cause socioeconomic impacts including economic losses, travel and energy disruptions, and fatalities (Dixon *et al* 2005, Field *et al* 2012, Singh *et al* 2024), garnering extensive media attention such as reports in the New York Times, Washington Post, and BBC and other major news agencies.

A key motivation of this study is the often-reported lack of decrease in the occurrence and strength of Northern Hemisphere (NH) midlatitude cold extremes in the face of AA. Although a significant body of work suggests that such cold extremes have remained approximately equally severe and frequent as several decades ago or even become more common (Cohen *et al* 2014, 2018, 2020, 2023, Overland *et al* 2015, 2021, Nygård *et al* 2023), other studies suggest that cold events have warmed more than have warm events (e.g. Screen 2014, Davy *et al* 2017, Sui *et al* 2020). Results are sensitive to the metrics, study period, region, season, and the height of temperature measurement above the ground (whether 1–2 m or higher).

Multiple studies support that AA favours the occurrence of midlatitude cold extremes in winter (Overland *et al* 2011, Francis and Vavrus 2012, Outten and Esau 2012, Mori *et al* 2014, Cohen *et al* 2021), although other work does not support such a link (e.g. Blackport *et al* 2022). The Arctic warming often corresponds with midlatitude cold anomalies over Eurasia and North America, associated with atmospheric blocking anticyclones (Cohen *et al* 2014, 2020, Overland *et al* 2015 2016, Ye and Messori 2020, Luo *et al* 2022, Cai *et al* 2024). Such a pattern has been labelled 'Warm Arctic Cold Continents' (Overland *et al* 2011). This correspondence does not imply the existence of a definite Arctic-midlatitude linkage, and such linkage can vary depending on different contemporaneous influences, jet-stream location and surface conditions; therefore, characterising Arctic-midlatitude linkages is a difficult task (Overland 2016). Furthermore, part of the observed AA in the last few decades is driven by internal variability that has enhanced Arctic warming while damping global warming (England *et al* 2021, Sweeney *et al* 2023). This internal variability features an internal surface air temperature trend pattern with warming in the Barents and Kara Seas and cooling over the tropical Eastern Pacific and Southern Ocean (Sweeney *et al* 2024). There is limited research on how such internal variability affects observed Arctic-midlatitude linkages. Despite such scientific uncertainties and challenges, identifying potential connections between the rapid Arctic change and extreme weather is instrumental to predicting the likelihood of these events with sufficient warning to allow emergency management organisations and decision-makers for infrastructure to prepare for adverse winter weather conditions.

The consequences of AA could be significant and widespread across the globe via changes in the jet stream (Francis and Vavrus 2012, 2015, Francis *et al* 2018, Moon *et al* 2022, Cohen *et al* 2014), storm tracks (Wickström *et al* 2020), the SPV (Cohen *et al* 2020, 2021), as well as changes in the ocean circulation (Bretones *et al* 2022, Polyakov *et al* 2023). Previous studies have linked the changing Arctic to cold spells (Honda *et al* 2009, Mori *et al* 2014, Cohen *et al* 2018, Zhang *et al* 2018a, Zhang *et al* 2020, Cohen *et al* 2021, Zhang *et al* 2022a, 2022b), snowfall (Cohen *et al* 2018, Bailey *et al* 2021) and extreme rainfall (Ma *et al* 2021, Chen *et al* 2021a) in the NH midlatitudes. However, this topic remains a central and controversial area of research and debate, balancing ideas of local forcing such as surface heating owing to sea-ice loss with natural variability. Uncertainty in causality arises from the 'tug-of-war' between global-warming-related atmospheric circulation changes in the tropics and the Arctic (e.g. Peings *et al* 2019). Assessment of relative and intermittent contributions by internal atmospheric chaotic variability, identification of cause and effect, and the lack of consensus between model and observational studies (Luo *et al* 2016, Sun *et al* 2016, Blackport *et al* 2019, Cohen *et al* 2020) complicate the issue.

A literature search via the Web of Science for 2020–2023 using *Arctic AND Midlatitude AND (Jet Stream OR Polar Vortex)* yields 75 references and a few more from other sources. This large number is indicative of

the importance, timeliness, and complexity of this topic. Multiple approaches to study Arctic/midlatitude connections have been applied, including statistical analyses of observational data and global coupled model (GCM) outputs, and targeted GCM simulations, to reveal causal connections between Arctic change and the winter tropospheric/surface response. Much of the evidence supporting an Arctic/midlatitude influence is based on observations, while results from GCMs are often conflicting (Cohen *et al* 2020). Seasonal or even monthly averages obscure individual sub-monthly events. Some researchers (e.g. McCusker *et al* 2016, Fyfe 2019, Screen and Blackport 2019, Blackport and Screen 2020, Dai and Song 2020) report little evidence for midlatitude impacts of the striking decline in Arctic sea ice, although these studies mainly examined responses to Arctic sea-ice loss alone rather than AA more generally, where the former misrepresents the vertical extent of warming and hence the atmospheric dynamical response: an example is Siberian blocking (Labe *et al* 2020). The need to investigate multi-model and single-model ensembles is broadly underscored (Elsbury *et al* 2021, Peings *et al* 2021, Xu *et al* 2021, Smith *et al* 2022, Ye *et al* 2024a). Studies focusing on dynamics highlight the interconnected roles of the stratosphere, jet-stream meanders, Rossby wave breaking, blocking, and non-linear interactions. Further work uses causality methods, with for example Samarasinghe *et al* (2019) using Granger and Pearl causality together with regression analysis to quantify a positive feedback between daily Arctic temperatures and North Pacific jet stream changes. Similarly, Kaufman *et al* (2024) using a causal inference framework deduced that positive weekly anomalies in Ural sea-level pressure resulted in Barents–Kara sea (BKS)-ice loss and central Eurasian cooling. Many analyses focus on the linkages between warm Arctic and cold midlatitude events, but connections have also been found between cold Arctic anomalies and warm winter events in midlatitudes, especially in Europe (Vihma *et al* 2020). Such a range of results confounds those who would like a single answer to follow the science and anticipate seasonal outlooks. Recognising multiple viewpoints and acknowledging intermittency of linkages reflect the current state of knowledge (Shepherd 2021, Smith *et al* 2021). Accumulated evidence suggests that recent trends in northern midlatitude winter cold events are due to a combination of influences, including both Arctic warming and interannual variability (Wallace *et al* 2012, Luo *et al* 2021, Outten *et al* 2023).

The purpose of this Review is to evaluate evidence from nonlinear blocking theory and a wide range of SPV (i.e. a mass of cold, cyclonically rotating air about 15–50 km high that encircles the Arctic during the cold season (AMS 2019)) excursions that influence winter CAOs, as well as to consider potential Arctic-midlatitude tropical teleconnections and evidence from large-ensemble climate model simulations of Arctic-midlatitude linkages. The SPV has been relatively under-studied in previous reviews of Arctic-midlatitude climate linkages that focus predominantly on the role of changes in the tropospheric polar jet stream, which is a flow of eastward-moving air driven by planetary rotation, latitudinal temperature differences and the conservation of angular momentum, which tends to lie south of the Arctic (e.g. Hall *et al* 2015). The Review is organised as follows. After this Introduction, in section 2 we consider characteristics of and trends in AA, CAOs and NH high-latitude blocking as such blocking provides a conduit of troposphere–stratosphere couplings and therefore Arctic-midlatitude linkages. Section 3 contains a summary of a nonlinear theory of blocking and its application to cross-latitude climate linkages. Section 4 presents a detailed discussion about the role of the NH SPV and, in particular, the extent to which its strength and movement (centre location and vortex orientation) southward over the NH continents provides a mechanism for enhancing regional CAOs. Disruptions in the SPV and stratosphere–troposphere interactions are crucial in consideration of Arctic-midlatitude climate linkages and associated winter weather extremes, considering that in winter the stratosphere and troposphere are frequently coupled through the propagation of waves both upwards and downwards (e.g. Baldwin and Dunkerton 1999, Baldwin *et al* 2021, Butchart 2022). Hence, to complement the literature review, section 4 includes new analyses on SPV displacement. Recent work suggests that influences on the Arctic from the tropics might connect onto the midlatitudes (e.g. Ding *et al* 2014), so in section 5 we discuss these potential teleconnections. Section 6 provides an evaluation of the evidence from ensembles of GCM simulations and what they reveal about mechanisms of Arctic-midlatitude climate linkages, and current limitations of such studies. Section 7 summarises and makes recommendations for further research.

## 2. AA, CAOs and blocking in midlatitudes

### 2.1. Characteristics of and trends in AA
Over the period 1980–2023 observed annual mean surface air temperatures in the Arctic have warmed about four times faster than the global mean; faster than predicted by climate models (e.g. Rantanen *et al* 2022, Ballinger *et al* 2023, Sweeney *et al* 2023). A recent study found removing internal variability using a machine learning method brings simulated and observed AA into agreement (Sweeney *et al* 2023). The region north of 60°N was on average 1.33 °C warmer for the annual mean, and 1.63 °C warmer for spring (March/April/May; these being the months following the seasonal maximum in sea-ice coverage), in
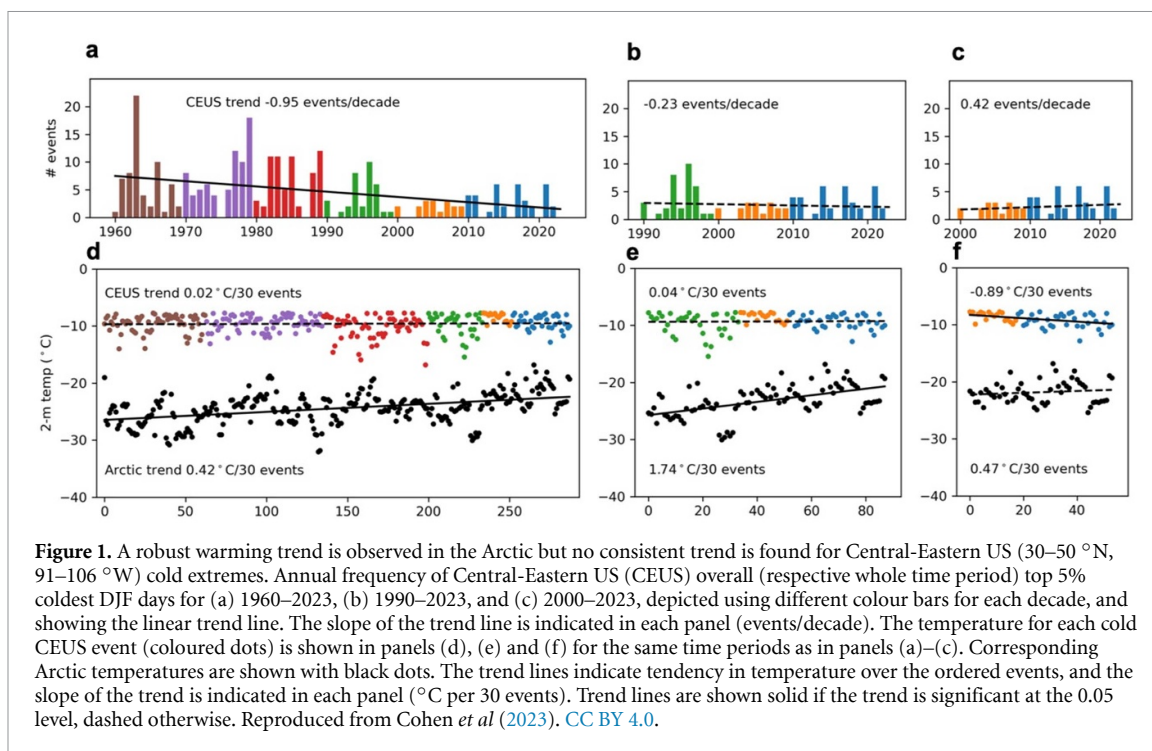
1991–2021 than in 1951–1980 (Wendisch *et al* 2023). Arctic warming is largest near the surface and also extends throughout the troposphere (Hall *et al* 2021, Ye and Messori 2021), producing a maximum in geopotential height surfaces at the tropopause (Francis and Vavrus 2015). AA arises from several climate feedbacks that act in combination, including the surface-ice albedo feedback, ice-ocean heat flux feedback (a warmer ocean under reduced sea-ice cover warms the overlying atmosphere), Planck feedback (where longwave emission increases with rising temperature), and the lapse-rate feedback (a stably stratified atmosphere results in greater warming near the surface) (Armour *et al* 2013, Pithan and Mauritsen 2014, Zhang *et al* 2018b, Hall *et al* 2021, Previdi *et al* 2021, Taylor *et al* 2022). Even in the absence of the surface-albedo feedback, AA still occurs due to changes in moisture transport together with a local greenhouse effect (Graversen and Wang 2009). Apart from the above-mentioned feedbacks, AA is also caused by changes in the meridional energy transport through an increase in latent energy transport that outpaces the cooling effect of a decreasing dry-static (i.e. poleward movement of internal and gravitational potential energy in the atmosphere) energy transport in a warming climate (Graversen and Burtu 2016, Hahn *et al* 2021). As well as being maintained through radiative forcing, AA is enhanced through persistent, frequent and intense synoptic episodes of poleward heat transport (Hall *et al* 2021), suggesting the importance of improving understanding of changes in the atmospheric polar jet stream and cross-latitude teleconnections (Henderson *et al* 2021). AA is related to a moistening of the central Arctic caused by a combination of increased evaporation from newly ice-free ocean areas and increased advection of mild and moist air by transient cyclones (Ma *et al* 2024), which can be deflected northwards by more frequent occurrences of Ural blocking (UB), for example, combined with the positive North Atlantic Oscillation (NAO) (Luo *et al* 2017) and Scandinavia-UB in early winter (Wendisch *et al* 2023).

## 2.2. Characteristics of and trends in CAOs

Extreme weather events, such as CAOs, exert substantial impacts on human health, energy consumption, agriculture, and wellbeing. Global warming is projected to increase some weather extremes—for example heatwaves, drought, and heavy precipitation events (Coumou and Rahmstorf 2012, Coumou *et al* 2015, Lin *et al* 2016, Na *et al* 2020, Qi *et al* 2022, Rogers *et al* 2022, Overland 2024)—but not severe winter weather such as CAOs and heavy snowfalls (Ashley *et al* 2020, Cohen *et al* 2020). Yet contrary to many GCM projections that predict a general and widespread decrease in cold extremes (Seneviratne *et al* 2021), recent weather extremes have included a lack of decrease or even an increase in CAOs and/or heavy snowfalls regionally across the NH since 1990 up to the recent past (Cohen *et al* 2014, 2018, 2020, Overland *et al* 2015, 2021). Work carried out using GCMs supports more likely and longer-lasting future CAOs over central Asia under continued 21st Century Arctic sea-ice loss (Francis 2015, Screen *et al* 2015), with a very large ensemble modelling study yielding more severe future Asian cold extremes in response to a stronger Siberian High and East Asian jet (Ye *et al* 2024a).

Cohen *et al* (2023) show that, despite the dramatic Arctic warming in the recent period, the temperature of cold extremes based on daily mean temperatures in populated regions of the NH midlatitudes has stayed nearly constant; that is, there has not been a corresponding moderation of midlatitude cold extremes associated with AA. However, the story is not straightforward. Clearly fewer cold records are being broken overall but recent CAOs continue to penetrate relatively far south into areas ill-equipped to deal with frigid temperatures—such as Texas, Florida, the Mediterranean and the Middle East—and their duration may be increasing in some areas (Francis 2015, Screen *et al* 2015). There is a clear divergence between Arctic temperatures, which are increasing rapidly, and the temperature of cold extremes in the central-eastern US, northeast Asia and even Europe, which have remained statistically unchanged (Cohen *et al* 2023). During 1960–2023, the frequency of cold extremes in those regions has decreased, although this trend is neutral during the more recent period of strong AA since 1990. Results for the central-eastern US are shown in figure 1. One recent period of extreme winter weather was the disruptive cold spells of January and February 2021 in Asia (Zheng *et al* 2021), Europe (DW.com 2021, Euronews.com 2021), and especially south-central US. The US southern plains cold wave of February 2021 may be unique in the observational record for the region based on the aggregate severity of the cold intensity, cold duration, southward cold extension, and widespread disruptive snowfall (Cohen *et al* 2021). As mentioned in the Introduction, other CAOs in January 2024 invaded the central US and northern Europe during an otherwise anomalously warm winter.

NH midlatitude CAOs and extremes are mainly produced by midlatitude atmospheric circulation patterns, i.e. deep troughs and changes in high-latitude blocking that are often related to the negative phase of the NAO, which is partly driven by internal atmospheric processes and does not necessarily require Arctic changes for its occurrence (Overland *et al* 2015, Luo *et al* 2016, 2019a, Sun *et al* 2016, Ye *et al* 2024b). For example, intense cold extremes still emerged over Eurasia during 1965–1976, an Arctic cooling period, and are mainly attributed to UB (Luo *et al* 2022). Because Arctic climate change is a relatively slow process compared to synoptic changes, it can be considered as a background condition that influences the likelihood

**Figure 1.** A robust warming trend is observed in the Arctic but no consistent trend is found for Central-Eastern US (30–50 °N, 91–106 °W) cold extremes. Annual frequency of Central-Eastern US (CEUS) overall (respective whole time period) top 5% coldest DJF days for (a) 1960–2023, (b) 1990–2023, and (c) 2000–2023, depicted using different colour bars for each decade, and showing the linear trend line. The slope of the trend line is indicated in each panel (events/decade). The temperature for each cold CEUS event (coloured dots) is shown in panels (d), (e) and (f) for the same time periods as in panels (a)–(c). Corresponding Arctic temperatures are shown with black dots. The trend lines indicate tendency in temperature over the ordered events, and the slope of the trend is indicated in each panel (°C per 30 events). Trend lines are shown solid if the trend is significant at the 0.05 level, dashed otherwise. Reproduced from Cohen *et al* (2023). CC BY 4.0.

of cold extremes. However, it is unclear how midlatitude cold extremes are directly linked to Arctic changes and what is the causal relationship. Furthermore, CAOs are influenced not only by large- and synoptic-scale drivers but also by local forcing, such as cloud radiative forcing, turbulent surface fluxes, and the structure of the atmospheric boundary layer (ABL). In northern Europe, cold near-surface anomalies are associated with relatively clear skies and low wind speeds (Sui *et al* 2020). The former enhances longwave cooling of the Earth's surface, while the latter reduces ABL turbulence, favouring strong surface-based temperature inversions (Sterk *et al* 2016).

### 2.3. Characteristics of and trends in NH high-latitude blocking

An atmospheric block is a quasi-stationary, persistent modification of the jet-stream flow that occurs at mid and high latitudes that typically lasts for one to a few weeks (e.g. Woollings *et al* 2018). Blocking events are associated with persistent weather conditions in the vicinity of the block that frequently leads to extreme weather events in midlatitudes, including winter CAOs (Hanna *et al* 2016, Woollings *et al* 2018, Overland *et al* 2021). The physical causes of blocking, and consequently how blocking responds to and influences climate change, are not well understood (Woollings *et al* 2018), especially in terms of connecting weather (daily) with climate (interannual) timescales. However, blocking, such as that over Greenland, the North Pacific and Barents/Kara seas may act as conduits between Arctic-amplified global warming and NH midlatitude jet-stream changes, although such linkages are complex and non-linear (Overland *et al* 2016). High-latitude blocking episodes are sometimes linked to, and may precede, SPV movement, disruptions or sudden stratospheric warmings (SSWs) (section 4). For example, a strong Greenland blocking episode in early December 2022, which was associated with severe weather impacts over the UK and central/eastern US, coincided with a weakening of the SPV and an intensifying Ural ridge (Lu *et al* 2023).

The conclusions from studies of how winter blocking may have changed over time can depend on the blocking metrics used (Woollings *et al* 2018). Consequently, we advocate using a multi-metric analysis approach. Waznah *et al* (2021), using long-running (1901–2010) Coupled Reanalysis of the 20th Century (CERA-20C) data (Laloyaux *et al* 2016), found no significant overall change in North Atlantic (north of 35 °N) blocking frequency from 1901 to 2010, although they did find some significant seasonal increases in blocking duration and intensity, such as more blocked days over Europe in spring and summer and more intense blocking over the Atlantic and Pacific in spring. They found no significant decreases in blocking intensity for any region. Li *et al* (2023a) applied three different standard and new blocking indices to European Centre for Medium-Range Weather Forecasts ERA-Interim reanalysis data (Dee *et al* 2011) for the 1979–2019 period; they identified increases in blocking frequency and intensity over the Urals and BKS in winter, over the northern North Pacific and east Siberia in spring, over west Greenland in summer, and over Europe, the North Atlantic and Norwegian Sea in autumn, along with decreases in a few areas. Woollings

*et al* (2018), using a hybrid reanalysis and blocking index approach for the period 1958–2012, found few areas of significant blocking frequency change for the winter season. A significant increase in the year-to-year variability of Greenland blocking in winter has been observed (Hanna *et al* 2015). Based on a two-dimensional potential vorticity-potential temperature blocking index, Tyrlis *et al* (2020) found a significant relationship between UB onset and subsequent central Asia cooling on interannual to decadal timescales, confirming previous findings.

How blocking events, especially in the cold season, may change has an important bearing on understanding the effects of AA on CAOs, as for example more Scandinavian and Greenland blocking episodes in winter favour more frequent, but perhaps less severe, CAOs over northern Europe and eastern North America (Vihma *et al* 2020). GCMs project an overall decline in blocking occurrence for the rest of this century, in line with an increase in the Northern Annular Mode (NAM)/Arctic Oscillation, but these projected trends have low confidence (Woollings *et al* 2018, Lee *et al* 2021). GCMs struggle to capture recent trends in blocking, for example the significant increase in Greenland summer blocking (Hanna *et al* 2018, Delhasse *et al* 2021).
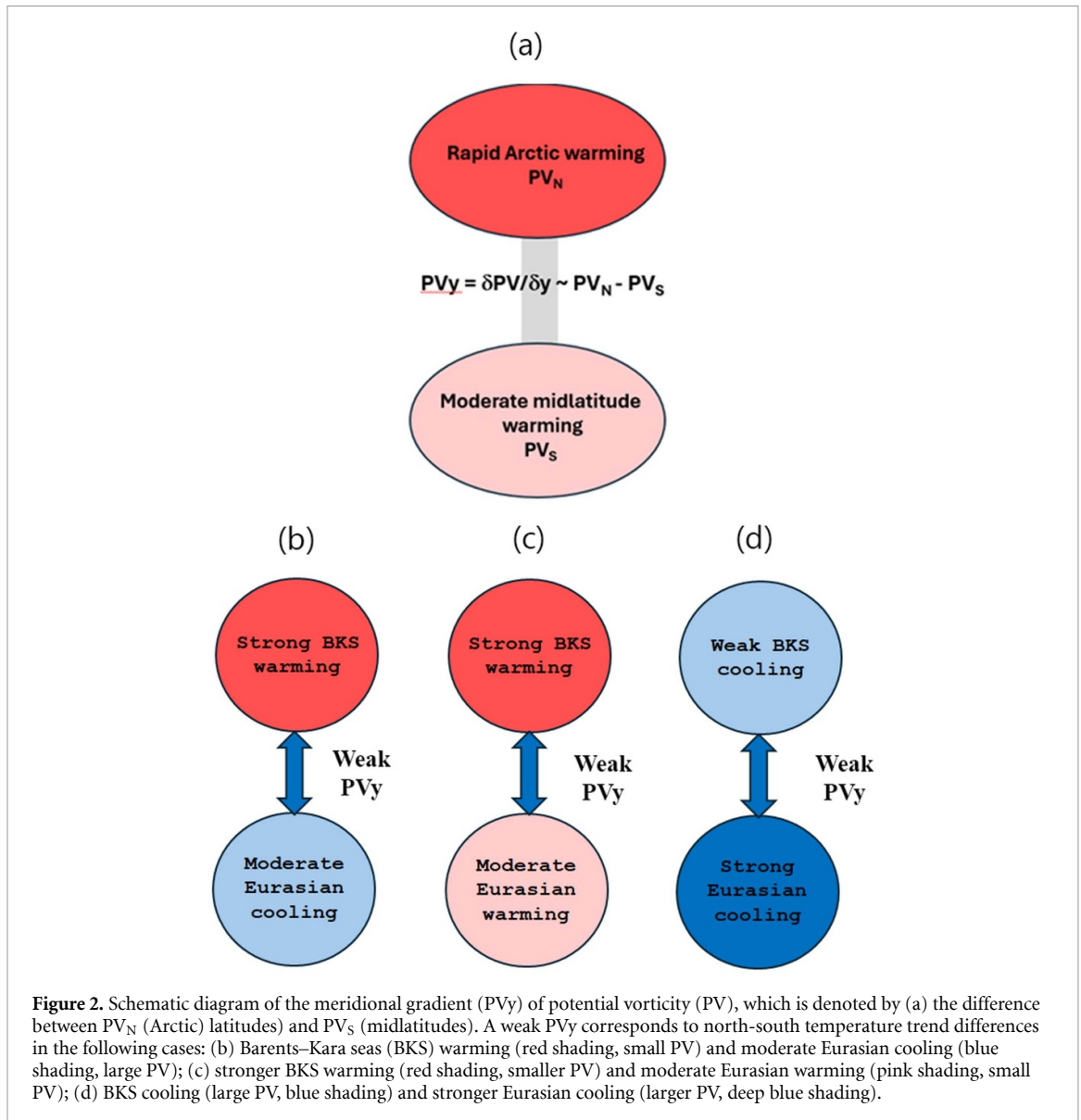
## 3. Non-linear theory of blocking and its application to Arctic-midlatitude weather linkages

Atmospheric blocking is a key conduit of Arctic/midlatitude weather linkages. Both blocking and linkages are intermittent and have preferred geographic locations and sub-seasonal duration ($\sim$10–20 d) (Overland *et al* 2015, 2016, 2021). A recent theory of blocking as an Arctic/midlatitude sub-seasonal weather bridge is the nonlinear multi-scale interaction (NMI) model (Luo *et al* 2019a, 2019b, 2023, Luo and Zhang 2020). The NMI model is based on synoptic-scale eddies, the blocking dipole feature, and the background zonal flow, all tending to possess the same low-frequency timescale (10–20 d) during their interaction. In this model, the blocking amplitude as a wave packet is described by an eddy-forced nonlinear Schrödinger equation (Luo 1991, 2000, Luo *et al* 2019a). The theory is time-dependent, invoking internal atmospheric variability as causality in the form of atmospheric eddy deformation, energy dispersion, and nonlinearity of the blocking system and eddy forcing. The evolution (lifetime, intensity, and movement) of blocking can be significantly influenced by the magnitude of background thermodynamic and dynamic atmospheric conditions, such as north-south potential vorticity gradients. This model is suitable for describing the NAO and Pacific North American patterns and the annular modes.

According to NMI theory, the lifetime of blocking is mainly determined by the meridional background potential vorticity gradient (PVy) (i.e. north-south gradient of the curvature of basic atmospheric features or meanders in the basic circulation). PVy can be expressed as $PVy = dPV/dy \sim PV_N - PV_S$ (figure 2(a)), where $PV_N$ ($PV_S$) represents the background PV over high latitudes (midlatitudes). The magnitude of PVy does not only depend on the value of $PV_N$ over the Arctic, but also on the value of $PV_S$ over northern midlatitudes. For a large-scale atmospheric system, anticyclonic (cyclonic) circulation or warming (cooling) corresponds to a low (high) background PV region (Luo *et al* 2019b). If a stationary large-scale geopotential ridge or warm anomaly in the troposphere appears in the NH, then the south side of this stationary ridge or warm anomaly corresponds to a reduced PVy in the troposphere.

When PVy is weaker, a blocking system tends to have weaker energy dispersion and stronger nonlinearity so that the block has a longer lifetime, a larger zonal scale, slower decay and lesser eastward movement (Zhang and Luo 2020). Thus, a weak PVy is a favourable condition for long-lived blocking events and persistent, intense and widespread midlatitude winter cold extremes or summer heatwaves. The west-east (zonal) movement of atmospheric blocking is associated with the background westerly wind, PVy, and the blocking amplitude. The magnitude of PVy can be considered a switch between strong zonal wind flow (strong PVy) where meteorological features such as storms rapidly propagate eastward, and weak zonal flow (weak PVy) where quasi-stationary and persistent meridional-wavy features such as blocking patterns are likely.

A weak PVy is shown for three cases in figures 2(b)–(d). As shown in figure 2(b), warming in high latitudes and cooling in middle latitudes of the troposphere corresponds to a small meridional gradient of the potential vorticity between high and middle latitudes or a weak PVy (which arises from a weaker $PV_N$ minus stronger $PV_S$). This represents the case of Arctic warming and mid-latitude cooling. If warming over the Arctic is stronger than that in northern midlatitudes, this corresponds to a weak PVy, as shown in figure 2(c). When the Arctic and midlatitudes are both cooling, this situation also corresponds to a weak PVy (figure 2(d)) if the cooling in midlatitudes is greater than the Arctic cooling, or if the background PV is larger in midlatitudes than in the Arctic. Thus, intense winter CAOs do not necessarily require Arctic warming (Luo *et al* 2019b) because Arctic warming is not necessary for producing a weak PVy. This explains the intermittent and uncertain relationship between the Arctic warming in connection with sea-ice decline and midlatitude cold extremes (Overland *et al* 2021). In particular, when Eurasian cooling is strong, PVy is also

**Figure 2.** Schematic diagram of the meridional gradient (PVy) of potential vorticity (PV), which is denoted by (a) the difference between $PV_N$ (Arctic) latitudes) and $PV_S$ (midlatitudes). A weak PVy corresponds to north-south temperature trend differences in the following cases: (b) Barents–Kara seas (BKS) warming (red shading, small PV) and moderate Eurasian cooling (blue shading, large PV); (c) stronger BKS warming (red shading, smaller PV) and moderate Eurasian warming (pink shading, small PV); (d) BKS cooling (large PV, blue shading) and stronger Eurasian cooling (larger PV, deep blue shading).

small, likely owing to the presence of snow cover, even when the BKS region is slightly cooler in winter (figure 2(d)). Thus, intense winter cold extremes depend on factors in addition to Arctic warming (Luo *et al* 2019b), even though Arctic warming overall favours cold extremes associated with blocking events.

According to results from the theoretical NMI model (Luo *et al* 2019a), there is a critical threshold of background PVy that determines the persistence of atmospheric blocking. When background PVy is sufficiently small atmospheric blocking becomes persistent in a fixed region, which favours intense, frequent and long-lasting midlatitude cold extremes. When PVy becomes even lower or negative, i.e. it is less than a certain threshold (which requires much stronger Arctic warming), atmospheric blocking becomes less persistent in a fixed region with stronger westward movement (Chen *et al* 2021b), therefore inhibiting midlatitude cold extremes. This suggests that very strong Arctic warming may tend to inhibit intense midlatitude cold extremes. However, a moderate Arctic warming that allows a small background PVy to not fall below the above-mentioned threshold is a favourable condition for midlatitude cold extremes. This leads us to infer that winter midlatitude cold extremes will be less frequent if winter Arctic warming becomes much stronger under future rapid warming scenarios. Under such scenarios, it is difficult for a small summer background PVy to reach a critical threshold because summer Arctic warming is not much stronger than in midlatitudes. Thus, intense, widespread and long-lasting heatwave events can still be observed. It is easy, however, for a small winter background PVy to reach a critical threshold. Thus, it is likely that future rapid Arctic warming will suppress winter cold extremes under high-emission scenarios because of a very small background PVy. For example, Hong *et al* (2024) used the CESM1 large ensemble dataset with RCP8.5

**Figure 3.** Blocking frequency is largest in regions of small meridional potential vorticity gradient. (a) DJF-mean Z500 (contour interval (CI) = 100 gpm) and meridional potential vorticity gradient PVy (colour shading; $10^{-6}$ PVU m$^{-1}$ where 1 PVU = $10^{-6}$ m$^{-2}$ s$^{-1}$ K kg$^{-1}$) on the 315 K isentropic surface; the thick black contour line represents 5500 gpm. (b) Horizontal distribution of DJF-mean blocking frequency (%; colour shading), as represented by the percentage of instantaneous blocking days with respect to the total days of a winter. These plots are based on ERA-Interim data (Dee *et al* 2011) and the represented period is 1979–2013. Adapted with permission from Luo *et al* (2019b). © American Meteorological Society. Used with permission.

emission scenarios to find that winter cold extremes exhibited a sharp decline. Figure 3(a) displays the mean winter (DJF) PVy as shading, which is calculated on the 315 K isentropic surface located between 300 and 200 hPa in latitudes north of 40 °N. The winter PV gradient is large over the North Atlantic Ocean and North Pacific Ocean midlatitudes where strong jet streams prevail. Weak background PV gradients exist in three main regions of high latitudes: one extending from Europe to the Barents Sea/Ural region, near Greenland, and in the western North Pacific Ocean. Regions of high blocking frequency are defined as the percentage of blocking days with respect to the total number of winter days (figure 3(b)). Blocking frequency is largest in regions of weak background PVy. PVy can be further influenced by regional positive surface temperature anomalies, topography such as the Ural mountains, and by sea-ice loss (Luo *et al* 2019b, Chen *et al* 2021b). The loss of Arctic sea ice or AA is only one factor that can increase the likelihood of weak PVy gradients that favour blocking and CAOs.

The PVy theory based on the NMI model reveals a positive feedback between UB and BKS warming or sea-ice decline (Luo *et al* 2019b). The background BKS warming or sea-ice decline can reduce PVy, maintaining UB and increasing its quasi-stationarity, which can result in severe and persistent CAOs over Eurasia and the further intensification (reduction) of BKS warming (sea ice). Clearly, there is a positive feedback between the BKS warming/sea ice loss and the persistent UB during the blocking period. In the NMI model, the large-scale meridional potential vorticity (PV) gradient associated with blocking events is $(PVy)_T = PVy + (PVy)_B$ (Luo *et al* 2019a), where PVy is the background PV gradient mainly determined by the climate state, and $(PVy)_B$ is the instantaneous PV gradient of the blocking scale part during the blocking periods which depends on the persistence, movement and intensity of blocking events. In this theory, the lifetime, intensity and movement of atmospheric blocking is dominated by the magnitude of PVy rather than the value of $(PVy)_B$. Although the BKS warming/sea ice loss is amplified by the UB and CAOs over Eurasia during the blocking period, this UB-induced BKS warming primarily results in more $(PVy)_B$ reduction rather than the reduction of PVy. As a result, the background PVy does not drop below the critical threshold. According to the winter classification of strong and weak winter PVy associated with background Arctic warming and cooling over the BKS, a weak (strong) PVy in mid-high latitudes of Eurasia corresponds to a long-lived (short-lived) UB with weak (strong) movement (supplementary information figures S1(a) and (b)). Such a small (large) PVy condition is induced by background BKS warming (cooling) (figures S1(c) and (d)), which tends to favour (suppress) Eurasian cold extremes (figure S1(e)) via increasing (decreasing) the lifetime, quasi-stationarity and zonal scale of UB.

In summary, the NMI theory importantly includes nonlinear internal atmospheric dynamics, the occurrence and location of blocking, and the sub-seasonal duration of events. As an example, Yao *et al* (2023) found that CAOs and snowstorms in North America and Eurasia were related to unusually weak PVy conditions and persistent Alaska and UB during November–December 2022.

**Table 1.** Different types of SPV disruption: typical examples, their characteristics and impacts. The SPV displacement and stretching examples are from this study, whilst the SPV split examples are from Butler et al (2020).

|  | SPV displacements | SPV stretching | SPV splits |
| --- | --- | --- | --- |
| Example(s) | 14–17 January 2005 | 11–20 February 2021<br>20–28 December 2022 | February 2018<br>January 2019 |
| SPV characteristics | SPV moves from pole towards north of North American and west Greenland region. | Warming of polar stratosphere is zonally asymmetric and is usually focused in North Pacific sector. | Often, but not always, associated with SSWs (two of the three main categories of SSW involve SPV splitting). |
| Impacts | CAO in eastern US—depends on strength and duration of SPV anomaly (see figures 4(a) and (b)). | Typically CAO in Canada and US east of Rockies (see figures 4(c)–(f)). | Frequently North American cold wave, sometimes with simultaneous cold wave in Eurasia. |

## 4. The SPV

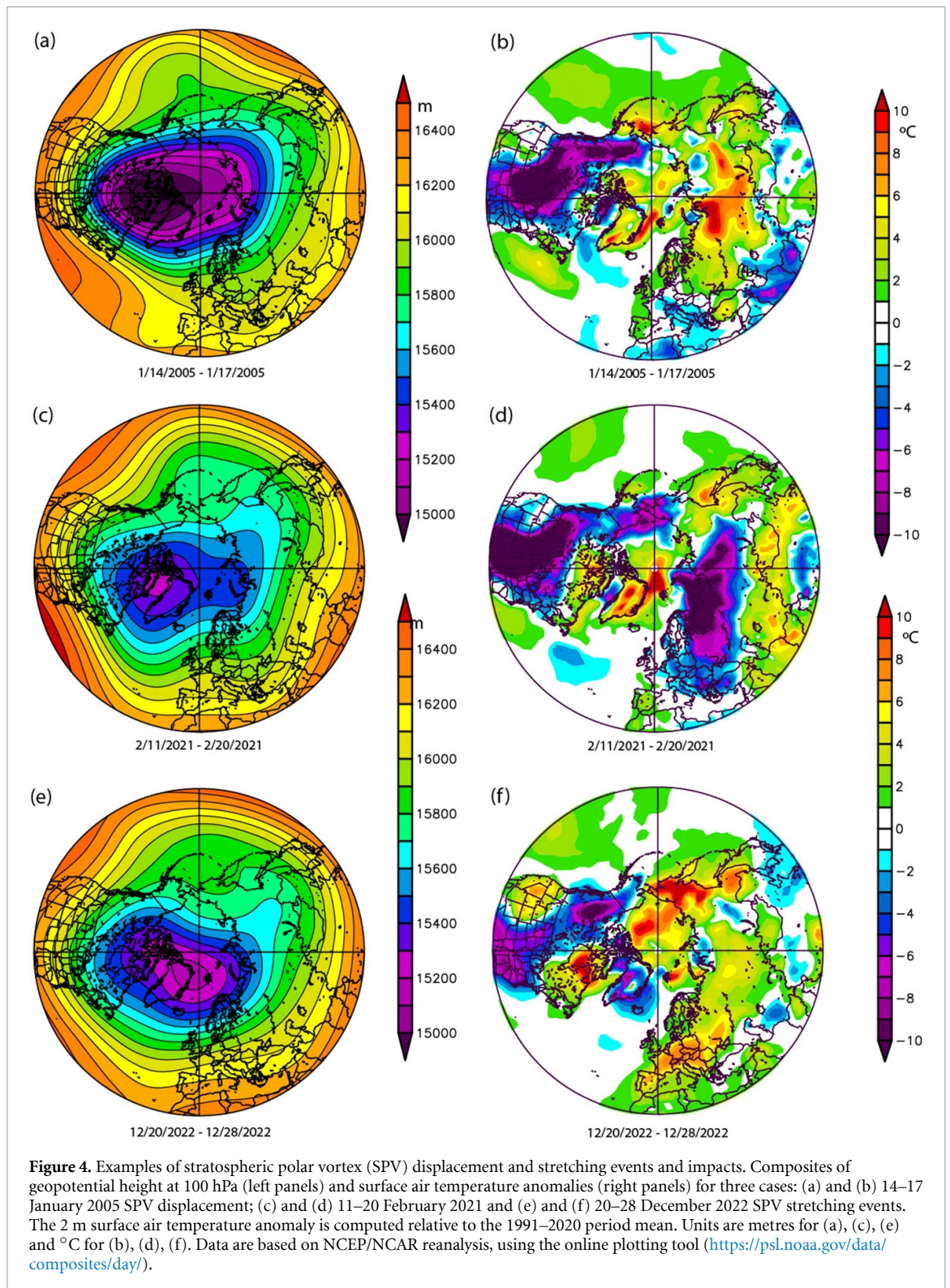### 4.1. Climatological SPV configuration and behaviour

Many recent studies have analysed the factors triggering cold spells, attributing them, at least in part, to SPV disruptions (e.g. Kretschmer *et al* 2018, King *et al* 2019, Kautz *et al* 2020, Huang *et al* 2021). When the SPV is in an extreme state, being anomalously weak or strong or shifted over continents, this leads to the modulation of large-scale tropospheric circulation patterns, and thereby winter weather in the midlatitudes. Weak SPV conditions, e.g. those associated with SSWs (4.2.3), favour the onset of the negative phase of NAO at the surface, often leading to colder weather over Northern Eurasia (e.g. Thompson *et al* 2002, Kidston *et al* 2015, Kretschmer *et al* 2018). Hoshi *et al* (2019) found, based on both observational and simulated data, that during weak SPV events under conditions of low sea ice in the BKS, upward Rossby wave propagation has a larger wavenumber 2 contribution, in contrast to a wavenumber 1 contribution dominating under large-extent sea-ice conditions. The weak SPV events in light-ice years are also followed by colder surface conditions particularly in Eurasia. Statnaia *et al* (2022) demonstrated that the probabilities of cold spells over northern Eurasia are systematically higher when there is a weak SPV at the initialization time. However, the usual negative NAO response after the weakening of the SPV occurs in only about two-thirds of cases (Domeisen *et al* 2020, Kolstad *et al* 2020). This variability may result in the overprediction of colder surface temperatures in northern Eurasia owing to the anticipation of the more common response, while an opposite surface signature might emerge instead. A comprehensive comparison of different SPV regimes is missing in the literature (Liang *et al* 2023).

Based on the five cluster patterns identified by Kretschmer *et al* (2018), we investigate different types of SPV patterns, summarised in table 1: displacement away from the North Pole (either towards Eurasia or North America), SPV stretching, and SPV splits (typically with one centre over eastern Eurasia and another over North America, and which are often associated with SSWs), and their surface impacts in relation to AA and Arctic-midlatitude linkages.

### 4.2. Types of SPV disruption

*4.2.1. SPV displacements*

One of the SPV disruptions is when the centre of SPV moves away from the North Pole: a SPV displacement. To track the movements of the SPV we use the 100 hPa geopotential height contour with a 15 000 m threshold. For North America, the domain encompassing 60–80 °N and 120–60 °W is of interest as previous studies showed that this is the region of action centre of cluster 2 (Kretschmer *et al* 2018). By examining the number of days when the daily 100 hPa geopotential height is below 15 000 m in this domain, one finds that the SPV is most active during January and February. By March cases with the SPV centre displaced to this region is reduced significantly. A case study of 14–17 January 2005 shows this strong connection: as the overall SPV moved, the centre of SPV stayed in the North American region. At the surface cold air gradually propagated from Alaska to the eastern US, resulting in an extreme CAO event on 16–18 January 2005. A composite plot of this case is shown in figures 4(a) and (b). We further examined the area occupied by the contour ⩽15 000 m on a daily basis. The 14–17 January 2005 example, with a maximum daily area of more than 3 million square km, stands out as having one of the largest such events. However, there are other cases when the SPV centre moved to the domain of interest, but no CAO occurred at the surface. This was due to

**Figure 4.** Examples of stratospheric polar vortex (SPV) displacement and stretching events and impacts. Composites of geopotential height at 100 hPa (left panels) and surface air temperature anomalies (right panels) for three cases: (a) and (b) 14–17 January 2005 SPV displacement; (c) and (d) 11–20 February 2021 and (e) and (f) 20–28 December 2022 SPV stretching events. The 2 m surface air temperature anomaly is computed relative to the 1991–2020 period mean. Units are metres for (a), (c), (e) and °C for (b), (d), (f). Data are based on NCEP/NCAR reanalysis, using the online plotting tool (https://psl.noaa.gov/data/composites/day/).

the SPV either being too weak or not lasting long enough. For the 33 years analysed (1990–2022), a dozen of these winters have a strong SPV positioned in the North American action centre. Smith and Sheridan (2019) also investigated the connection of CAO events with stratosphere and tropospheric polar vortex activities. They divided the winter (November to March of the following year) into five 28 d periods. They found that an off-centred, strong polar vortex increased in frequency during Weeks 2 and 3 in period 3 (27 December to 24 January). They also showed that both a strong, off-centred polar vortex pattern over the Beaufort Sea (T6) and weak polar vortex patterns (T1 and T4) were favoured 3–4 weeks in advance of CAOs. The pattern T6 is similar to what we show in figure 4(a).

### 4.2.2. SPV stretching

During SPV stretching events the warming of the polar stratosphere is zonally asymmetric, with the warming focused on the North Pacific side of the Arctic, usually centred near the dateline and Alaska. The SPV can remain weak or strong, as measured by polar cap geopotential heights (PCHs) and/or zonal-mean zonal wind and is often displaced a little off the North Pole towards the North Atlantic side of the Arctic, typically towards Greenland. Stretched SPVs are usually forced by an amplified standing wavenumber two in the troposphere where the excited upward wave energy is reflected off the SPV rather than absorbed, which limits the amount of polar stratospheric warming. Wave reflection off the upper stratosphere occurs rather than absorption when upwelling energy from the troposphere encounters a reflective layer (where the zonal winds in the stratosphere decrease with height or as marked by strong static stability in the lower stratosphere) (Messori *et al* 2022, Weinberger *et al* 2022). When a reflective layer is encountered, the warming in the polar stratosphere is focused on the location of reflection (typically in the North Pacific), leading to asymmetric warming of the polar stratosphere. In contrast, other cases show wave energy being absorbed when the upwelling energy can propagate deep into the stratosphere when no reflecting layer is encountered, typically when zonal winds do not decrease with height. Full absorption of the wave energy in the polar stratosphere leads to widespread and more zonally symmetric warming.
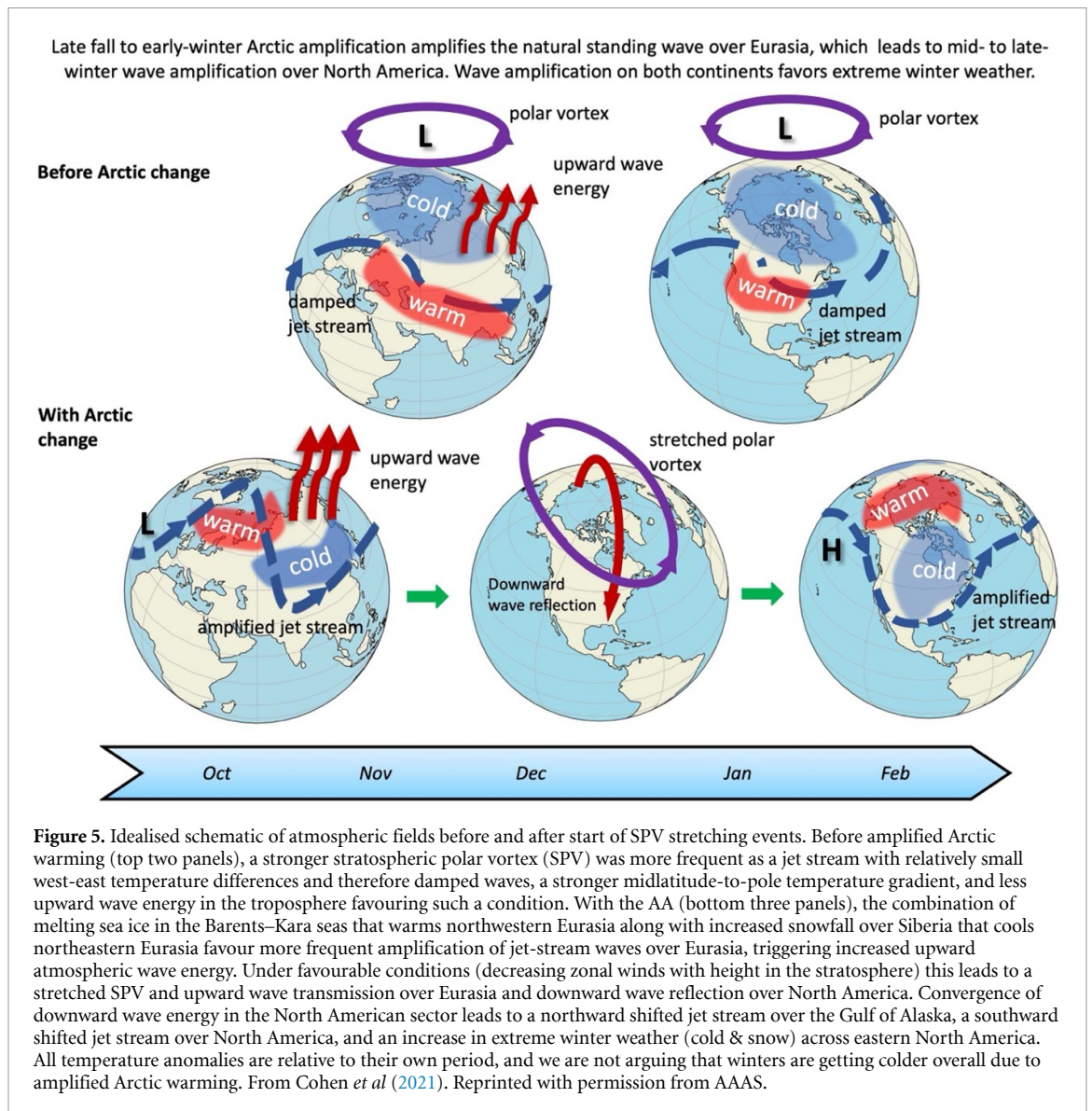
Kretschmer *et al* (2018) used machine learning to identify two dominant patterns of increased lower stratospheric geopotential heights over the polar cap, representing a weak SPV. The first pattern is the well-known SSW (4.2.3), leading to a negative phase of the NAO along with CAOs over northern Eurasia. The second pattern is zonally asymmetric and is linked to downward reflected planetary waves over Canada followed by a negative phase of the Western Pacific Oscillation and cold spells in Canada and the US east of the Rockies, such as during 11–20 February 2021 (figures 4(c), (d)) and 20–28 December 2022 (figures 4(e) and (f)). During these events the SPV elongates and is therefore referred to as a stretched SPV. When studying North American cold spells, it is crucial to consider vortex stretching forced by reflection of wave energy from the troposphere (Cohen *et al* 2021, Messori *et al* 2022). Although stretching events persist on average for days to up to 2 weeks, during October through February, they importantly explain a much larger part of North America's seasonal temperature variability than other weak SPV—SSW states.

In a follow up study, Cohen *et al* (2021) demonstrated that SPV stretching events have accelerated in the era of AA. As seen in figure S2, cluster 4, which represents SPV stretching events, is associated with cold temperatures in eastern North America and is the SPV pattern that is increasing the fastest in terms of annual frequency. Climate change in general, but especially AA, is favourable for forcing these events. A generalised timeline of the significant atmospheric features is outlined in figure 5 beginning with Ural ridging, followed by North Pacific ridging and ending with North American and East Asian cold events. It is argued that warming in the Barents–Kara and Chukchi–Bering seas owing to sea ice melt favours tropospheric ridging/high pressure in these regions (Kug *et al* 2015, Tachibana *et al* 2019, Cohen *et al* 2020, Overland *et al* 2021). Autumn Siberian snowfall has also been increasing (Wegmann *et al* 2015), favouring downstream troughing over East Asia. This pattern of ridging in the Urals/BKS region and troughing in East Asia strongly projects onto the tropospheric pattern favourable for forcing SPV stretching that often delivers extreme cold to Canada and the US. This interpretation is supported by GCM sensitivity experiments forced with increased Eurasian snow cover and decreased BKS ice, where the atmospheric response is an increase in SPV stretching events with troughing and colder temperatures across Asia and North America one to two months following the introduction of Arctic forcing (Cohen *et al* 2021).

### 4.2.3. SSWs

A SSW, the state of an extremely weakened SPV, as measured by anomalous PCHs and the zonal-mean zonal wind at 10 hPa and 60 °N, is characterised by a rapid and zonally symmetric increase in polar stratospheric temperature and an abrupt decrease in circumpolar zonal wind. SSWs are forced by amplified standing waves with wavenumbers one or two in the troposphere that excite upward wave energy. The absorption of this anomalous wave energy results in the dramatic warming of the polar stratosphere observed during SSWs.

SSWs can be categorised into multiple types depending on the shape of vortices: displacement, describing the SPV migration away from the pole, or splitting in which the SPV separates into two smaller vortices (Charlton and Polvani 2007, Cohen and Jones 2011). Choi *et al* (2019) further classified SSW events into three types based on the vortex shape before and after the onset date of the warming event: displacement–displacement (DD), displacement–split (DS), and split–split (SS). Figure S3 displays characteristic features of these three types of SSWs. The DD SSW type is characterised by a single displaced SPV with a wave-1 pattern throughout the SSW period. Before the onset of the SSW event, both DS and DD types show almost the same wave-1 pattern featuring a vortex displaced from its climatology. In the DS type, however, after the SSW onset, the SPV splits into daughter vortices that drift southward over Eurasia and

**Figure 5.** Idealised schematic of atmospheric fields before and after start of SPV stretching events. Before amplified Arctic warming (top two panels), a stronger stratospheric polar vortex (SPV) was more frequent as a jet stream with relatively small west-east temperature differences and therefore damped waves, a stronger midlatitude-to-pole temperature gradient, and less upward wave energy in the troposphere favouring such a condition. With the AA (bottom three panels), the combination of melting sea ice in the Barents–Kara seas that warms northwestern Eurasia along with increased snowfall over Siberia that cools northeastern Eurasia favour more frequent amplification of jet-stream waves over Eurasia, triggering increased upward atmospheric wave energy. Under favourable conditions (decreasing zonal winds with height in the stratosphere) this leads to a stretched SPV and upward wave transmission over Eurasia and downward wave reflection over North America. Convergence of downward wave energy in the North American sector leads to a northward shifted jet stream over the Gulf of Alaska, a southward shifted jet stream over North America, and an increase in extreme winter weather (cold & snow) across eastern North America. All temperature anomalies are relative to their own period, and we are not arguing that winters are getting colder overall due to amplified Arctic warming. From Cohen *et al* (2021). Reprinted with permission from AAAS.

North America in a wave-2 pattern. In the SS type, a wave-2 pattern persists throughout the SSW period, although the centre of action is displaced slightly after the onset.

Figures 6 and S4 display the surface response to SPV types for pre-SSW and post-SSW periods. For the case of DD and DS types, surface temperature responses are opposite before versus after the SSW, with a negative anomaly over Eurasia and a positive anomaly over North America before SSW, and vice versa. The temperature response, however, is more prominent in midlatitudes for the DS type after the SSW onset, with a positive anomaly over Eurasia and a negative anomaly over North America. In the SS type, both Eurasia and North America tend to experience colder-than-normal weather.

In the context of climate change, a question is whether the proportion of SSWs associated with cold weather extremes will vary and whether the magnitude and nature of any surface impacts will change. There is considerable skill in forecasting extreme weather following an SSW, with less certainty concerning the low-or-little impact SSWs (Knight *et al* 2021). Recent research has identified that a significant proportion of SSWs are not associated with the canonical SSW surface anomaly pattern (cold eastern US, warm Baffin Bay, cold Eurasia, warm middle east) (Karpechko *et al* 2017, Domeisen 2019, Afargan-Gerstman and Domeisen 2020. Hall *et al* 2022). There is considerable decadal variability in SSWs, these being most active around 2002, but studies disagree on recent (last few decades') long-term trends from the observed record. Li *et al* (2023b) found significant increases in SSW duration and strength from 1981–2020 using ERA5 reanalysis and radio occultation data. This is in agreement with Zhang *et al* (2021) who used NCEP/NCAR reanalysis data. However, Li *et al* (2024) found no significant overall trends in SSW duration and strength from

**Figure 6.** Schematic diagram of surface temperature and polar vortices during pre-warming (top row) and post-warming (bottom) periods for different types of sudden stratospheric warming (SSW) events. (a) Displacement–displacement (DD) type; (b) displacement–split (DS) type; and (c) split–split (SS) type. The circles with holes in the centre represent the SPV, and the filled circles represent surface temperature. The grey circle with a hole in the centre indicates the climatological SPV during winter, while the blue circles illustrate the shape and position of the polar vortex after the occurrence of SSW.
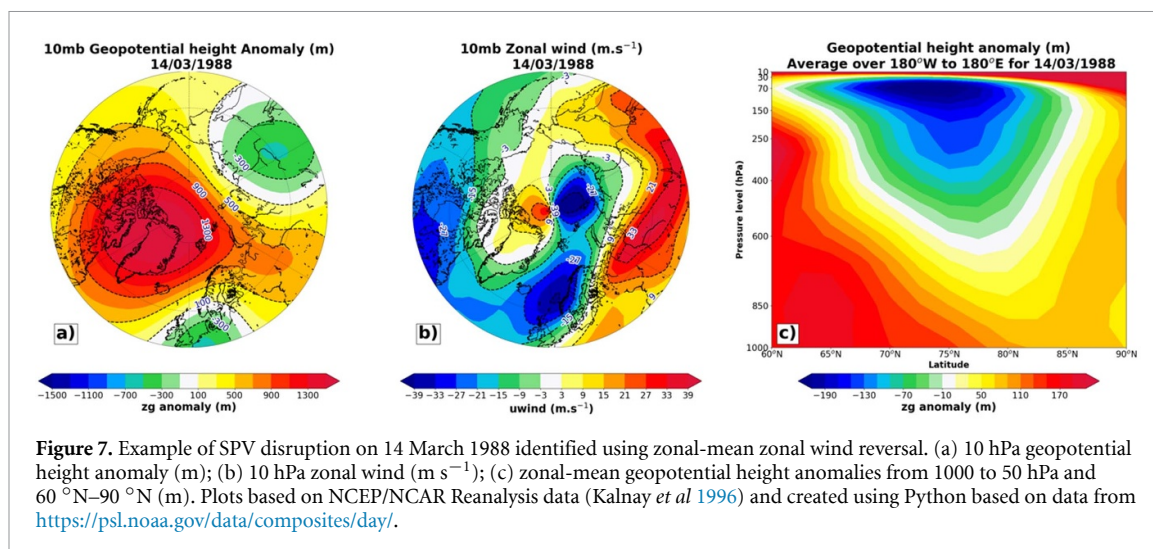
1980–2020, also based on ERA5 data. Attention is needed to reconcile these differences in the literature. Furthermore, there is little consensus concerning future changes in SSW frequency: CMIP6 models show divergent results (Ayarzaguena *et al* 2020).

There is large inter-event variability in temperature anomalies over the 60-day period following SSW onset (figure S5). For example, the warmest third of SSWs ('warm-impact events') are actually associated with positive temperature anomalies over the British Isles, and are not associated with the NAO, whereas the coldest third ('cold-impact events') are associated with negative British Isles temperature anomalies and a negative NAO (Hall *et al* 2023). The canonical 4-node temperature anomaly pattern over the NH is seen based on ERA5 data with cold and neutral SSW events, but not with the warm-impact events (figures S6(a)–(c)). An average over all SSWs conceals the surface impacts of the warm-impact events, instead producing the canonical pattern. The positive temperature anomalies over Europe associated with these warm-impact SSWs are also reproduced by CMIP6 models (Hall *et al* 2023) (not shown).

If the zonal-mean polar cap height anomalies are compared for warm- and cold-impact SSW events, the warm-impact events appear not to link to the troposphere as clearly, and in addition there are tropospheric precursors that distinguish the two types of event (figures S6(d) and (e)). This might be because the troposphere contributes to the magnitude of the SSW's surface impact, boosting it to the 'warm-impact event' category (see section 4.3). This supports the findings of White *et al* (2019) who suggest tropospheric wave activity is, on average, larger preceding the downward-propagating SSW, using a chemistry-climate model. However, only around two thirds of such events propagated to the surface in their experiments, and a large number of events is required to determine significance, so the result can only be used probabilistically.

Black and McDaniel (2004) identified that downward propagation of SSW depended on the pre-existing tropospheric state. The strength of high-pressure patterns over the Ural region (UB, e.g. Luo *et al* 2016, Peings 2019) is a well-known precursor to SSWs, and a Pacific signal is also found to influence the downward response (Afargan-Gerstman and Domeisen 2020). Future changes in UB under climate change will be important for determining changes in SSW frequency, particularly those associated with strong surface impacts. UB has a complex and contested association with other factors that may change under global warming, such as BKS ice extent and Siberian snow cover (Tyrlis *et al* 2017, Peings 2019, Cohen *et al* 2021, Chen *et al* 2021b, Peings *et al* 2023).

**Figure 7.** Example of SPV disruption on 14 March 1988 identified using zonal-mean zonal wind reversal. (a) 10 hPa geopotential height anomaly (m); (b) 10 hPa zonal wind (m s$^{-1}$); (c) zonal-mean geopotential height anomalies from 1000 to 50 hPa and 60 °N–90 °N (m). Plots based on NCEP/NCAR Reanalysis data (Kalnay *et al* 1996) and created using Python based on data from https://psl.noaa.gov/data/composites/day/.

### 4.3. Metrics to identify SPV disruptions

SPV disruptions—SSWs, stretching, splits, and displacements—are typically identified by reversals in the zonal-mean zonal wind at 10 hPa and 60 °N, as well as by average temperature or height anomalies at 10 hPa north of 60 °N. On many occasions, however, these metrics fail to detect disruptions because of hemispheric asymmetries, e.g. in the case of a weak-SPV identified by Cohen and Jones (2011) for 14 March 1988 based on a 10 hPa zonal-mean zonal wind reversal, figure 7. Moreover, variations in the troposphere can have dominant influences on upper-level heights, as shown in figure 7, implicating disruptions that may actually result from positive tropospheric height anomalies rather than stratospheric anomalies.

We propose and demonstrate a new metric to identify SPV disruptions that isolates stratospheric behaviour rather than conflating anomalies in both the stratosphere and troposphere. We base the new detection technique on daily 50–10 hPa thickness anomaly fields during mid/late winter (JF) with no zonal averaging. We employ a hierarchical clustering technique to identify characteristic spatial patterns in daily thickness fields north of 30 °N from 1979 to 2022 (figure S7(a)).

Resulting patterns indicate a variety of SPV configurations that differ markedly from the canonical circular, symmetrical SPV, suggesting a spectrum of conditions that could be described as disrupted. These patterns stand in contrast to those illustrated in Cohen *et al* (2021) that depict a nearly baroclinic stacking of height anomalies at 500 and 100 hPa. The nearly identical patterns at these two levels suggest the stratospheric configurations used to identify disrupted SPV conditions by these researchers include a substantial contribution from the troposphere. As polar tropospheric heights inflate with increasing AA, therefore an increased frequency of patterns depicting positive 100 hPa height anomalies would be expected, while changes in the stratosphere itself may exhibit a completely different behaviour, as illustrated in figure 7.

In figure S7(b) we present the temporal change in frequency of each pattern and fields of corresponding variables. Using this stratosphere-focused metric, we find that cluster #7—which represents a strong, north-pole-centred SPV—has become more common in recent decades, consistent with a cooling stratosphere owing to increasing radiative loss from greenhouse gases. This trend is opposite for the corresponding 100 hPa pattern shown in Cohen *et al* (2021), suggesting the trend based on 100 hPa heights may be influenced by tropospheric changes rather than variability in the stratosphere alone.

Cluster #7 is associated with predominant positive anomalies in 2 m temperatures across the NH (figure S7(c)), consistent with general observations of surface warming during strong SPV periods. The most disrupted pattern #5, however, is associated with anomalous cold over much of North America, indicating that cold spells are favoured in North America when a lobe of the SPV extends southward over the continent. Clusters #1 and #9 favour northerly winds from the Arctic into Siberia, resulting in negative 2 m temperature anomalies across northern Asia. Figure S7(d) displays an analysis of vertical wind profiles from 50–10 hPa for each cluster, colour-coded according to phase of the quasi-biennial oscillation (QBO). It is clear that zonal-mean zonal winds at 10 hPa do not necessarily indicate the state of the SPV. For example, nodes #2 and #7 depict strong SPV states, yet only #7 has strong westerly winds at 10 hPa. Moreover, highly disrupted SPVs such as those in #5, #8, and #10 exhibit both positive and negative wind anomalies.

In summary, we propose that an informative and accurate method to assess the state and behaviour of the SPV is based on stratospheric thickness anomalies rather than total troposphere–stratosphere height

anomalies or zonal-mean zonal winds. Positive height anomalies at 100 or 30 hPa may be caused by inflated tropospheric heights, which are known to be increasing as amplified Arctic warming continues.

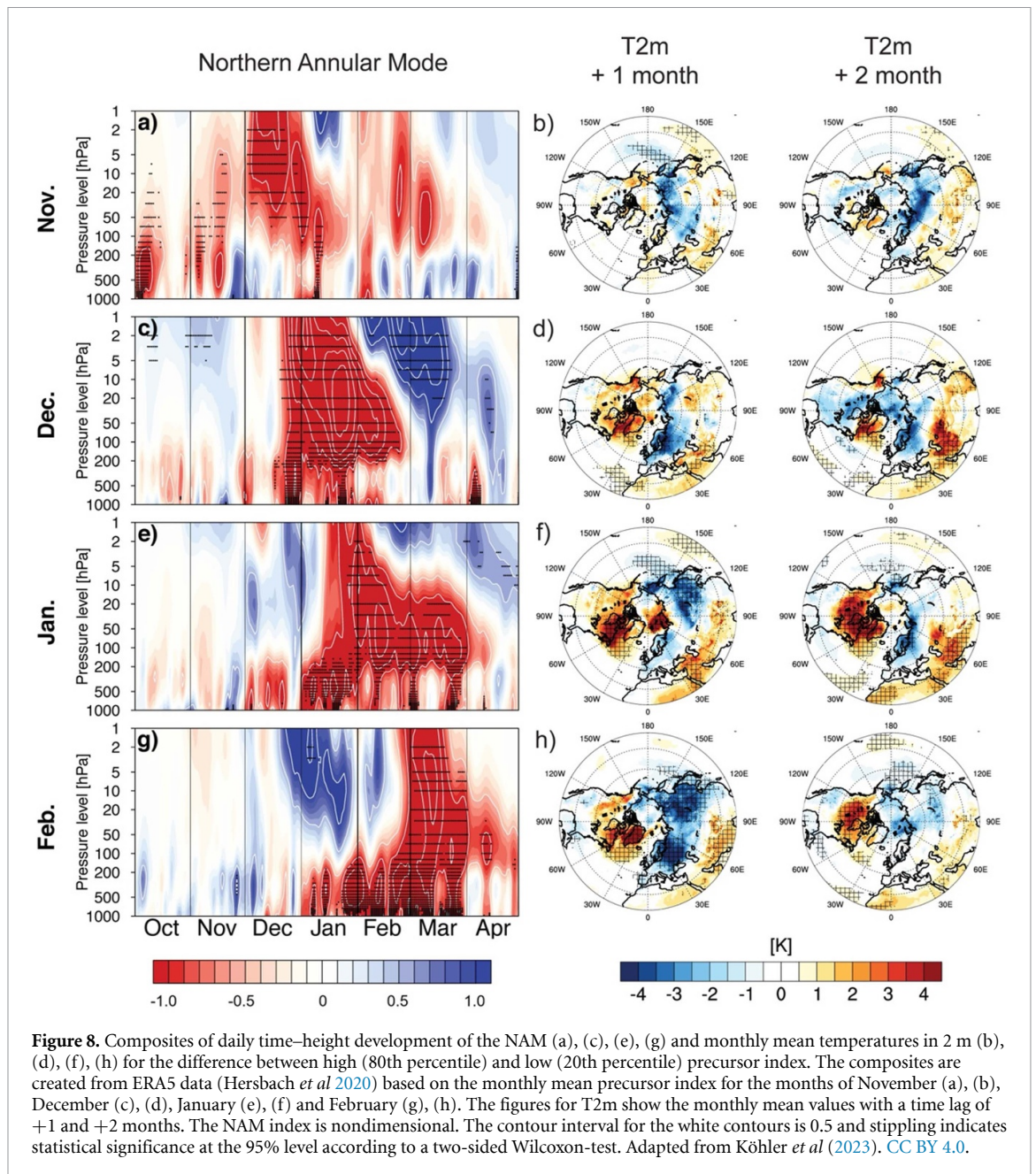### 4.4. Precursor conditions to SPV disruptions

The robust but highly intermittent stratospheric pathway for Arctic-midlatitude linkages can dynamically link AA and sea-ice loss to changes in midlatitude circulation patterns in late winter (Kim *et al* 2014, Nakamura *et al* 2015, 2016, Jaiser *et al* 2016, 2023, Cohen *et al* 2020, Siew *et al* 2020): early winter blocking in the Scandinavian/Ural region thereby plays an important role in triggering anomalous vertical wave propagation into the stratosphere, where subsequent wave breaking can lead to a disruption of the SPV. Such vortex disruptions are often accompanied by strong downward influences on the large-scale tropospheric circulation, favouring the negative phase of the Arctic Oscillation, a wavier jet stream, and anomalous CAOs in the midlatitudes. Although this pathway has received attention in literature, the sensitive precursor regions in the troposphere are not clearly defined, and the involved timescales of the pathway are frequently obfuscated by monthly mean data or averaging over fixed time lags.

To investigate these precursor mechanisms we regress daily winter (NDJF) mean sea-level pressure (MSLP) as a function of longitude onto the NAM at 10 hPa and as a function of time—a method based on Köhler *et al* (2023). Figure S8 demonstrates that MSLP in winter can be a predictor for the NAM at 10 hPa. In accordance with Garfinkel *et al* (2010), two areas exhibit significant regressions: the extended Ural region and the greater Aleutian low extending from the Sea of Okhotsk to the Rocky Mountains. The negative regression in the Ural region indicates that a high (low) pressure anomaly in this region is connected to a negative (positive) NAM at 10 hPa, and thus a weakened (strengthened) SPV during the following 60 d. The strongest influence of the MSLP on the polar vortex manifests after nearly 30 d. The positive correlation in the extended Aleutian low region, indicates that a strengthening (weakening) of the Aleutian low is associated with a weaker (stronger) SPV with a lag of 5–45 d, and a maximum after just under 20 d. Whereas the Ural region can play an important role in dynamically connecting changes in the BKS to the SPV, the Aleutian low region is an important link between El Niño Southern Oscillation (ENSO) and the SPV (e.g. Garfinkel and Hartmann 2008). Moreover, most CMIP (5 & 6) models project a future deepening of the Aleutian low in winter (Gan *et al* 2017, Giamalaki *et al* 2021, Chen *et al* 2021c) that could contribute to a future weakening of the SPV. A simple precursor index, consisting of the detrended MSLP difference between the Urals (45 °N–80 °N and 30 °E–100 °E) and the extended Aleutian region (5 °N–80 °N and 160 °E–100 °W), is strongly correlated with the strength of the SPV in the following one to two months (Köhler *et al* 2023). The positive phase of the index is related to a constructive interference with the climatological wave-1 pattern, as anomalously high pressure in the Ural region and anomalously low pressure in the Aleutian region are both related to an increase in the tropospheric wave-1 forcing.

The coupling of tropospheric pressure anomaly patterns to the strength of the SPV involves vertical propagation of planetary waves, which can be quantified by the vertical component of the Eliassen-Palm flux (EP flux). To investigate the spatial patterns and timescales of these vertical coupling processes, figure S9(a) demonstrates how the MSLP projects onto the vertical component of the EP flux at 100 hPa. Positive (negative) MSLP anomalies in the Ural region induce a positive (negative) vertical EP flux anomaly at 100 hPa—with maximum regression coefficients after 2–3 d at approximately 40 °E. The intensity of this positive relation weakens, while it broadens regionally at longer timescales up to 25 d. The effect of the Aleutian MSLP on the EP flux is less long-lasting with a nearly instantaneous maximum effect and a significant negative regression for up to 15 d.
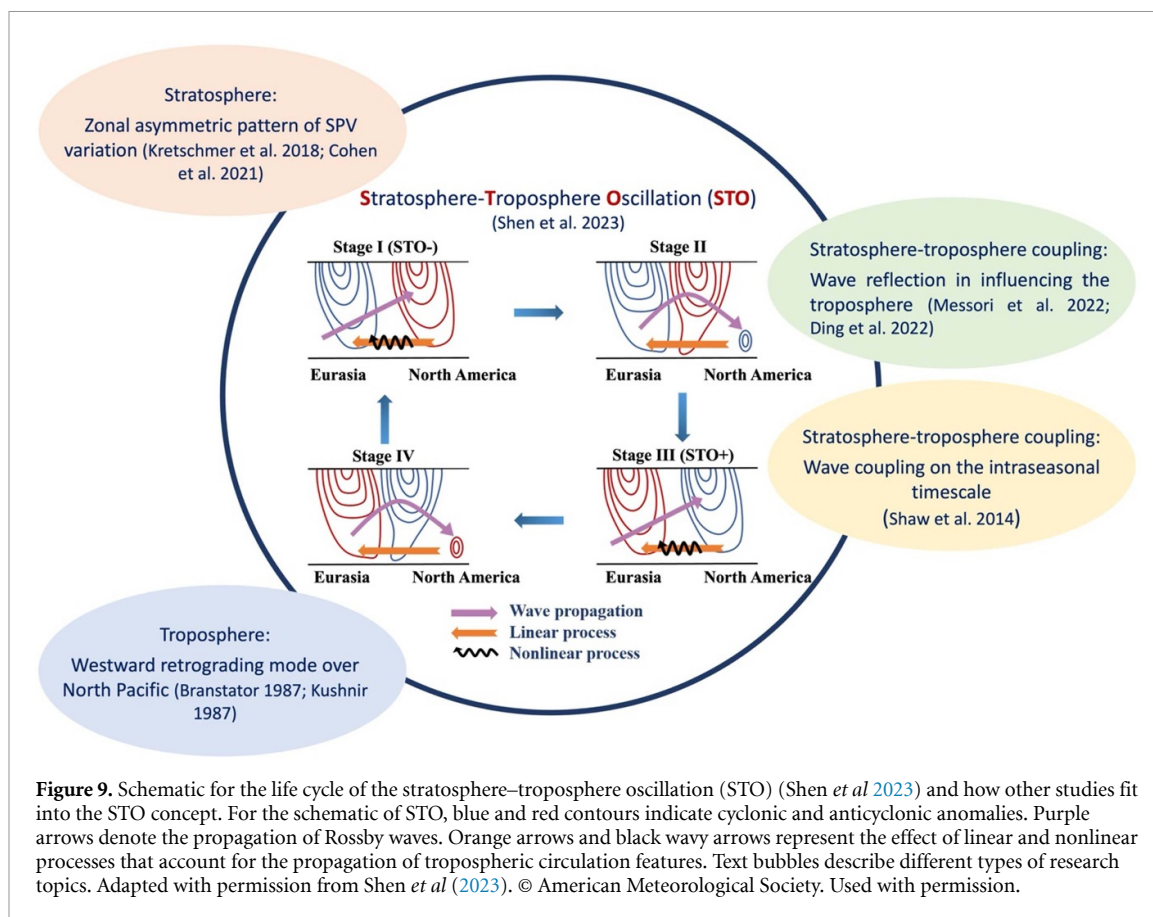
To further investigate the timescales of the influence of wave activity on the strength of the SPV, the vertical component of the EP-flux at 100 hPa is regressed onto the meridional mean geopotential at 10 hPa as a function of longitude and time in figure S9(b). The dominantly positive regression demonstrates that a positive (negative) EP-flux anomaly is related to a positive geopotential anomaly. The signal originates in the region of the stratospheric Aleutian high and extends over all latitudes in time, which—in the case of a vortex weakening—would be a typical vortex-displacement-type anomaly. The largest signal in the geopotential is visible after 10 d at 100 °E. However, the significant signal over Europe can last up to 50 d after the EP-flux anomaly. The comparison of the two figures demonstrates that stratospheric processes (Fig. S9b) have a larger contribution to the time lag in troposphere–stratosphere coupling (cf figure S8) than do the tropospheric processes.

To quantify the downward influence of stratospheric anomalies that are induced by tropospheric precursor patterns, we create composites of the NAM based on the earlier defined precursor index (cf figure 8). The NAM composite differences between years with a high and a low index in the months November–February illustrate the potential of tropospheric precursors for the subseasonal-to-seasonal prediction, as the stratosphere exhibits very strong NAM anomalies 2 months following the original tropospheric pressure anomaly. Similar to the original 'dripping-paint plots' by Baldwin and Dunkerton

**Figure 8.** Composites of daily time–height development of the NAM (a), (c), (e), (g) and monthly mean temperatures in 2 m (b), (d), (f), (h) for the difference between high (80th percentile) and low (20th percentile) precursor index. The composites are created from ERA5 data (Hersbach *et al* 2020) based on the monthly mean precursor index for the months of November (a), (b), December (c), (d), January (e), (f) and February (g), (h). The figures for T2m show the monthly mean values with a time lag of +1 and +2 months. The NAM index is nondimensional. The contour interval for the white contours is 0.5 and stippling indicates statistical significance at the 95% level according to a two-sided Wilcoxon-test. Adapted from Köhler *et al* (2023). CC BY 4.0.

(2001) and the multiple reproductions of their figure, the stratospheric NAM anomalies penetrate back into the troposphere and amplify at the surface, thus favouring the negative phase of the NAM. However, in this case, the NAM events were not selected using stratospheric criteria but only the MSLP difference between the Ural and the extended Aleutian region, thereby making use of the predictive power of these precursor regions. The NAM anomalies tend to be strongest in mid-winter, and the time lag between the precursor anomaly and the stratospheric NAM anomaly tends to increase towards the end of winter, but the overall signal remains the same throughout winter. The surface impact is visualised by creating 2 m-temperature composites for the 2 months following the original anomaly in the precursor index—once again these composites are based on the difference between years with a high and a low precursor index. The temperature impact at the surface in month one and two after the precursor anomaly is as expected from a negative NAM signal: lower temperatures over Eurasia and parts of the North American continent, along with higher temperatures in the Baffin Bay area, North Africa and the Middle East. This surface impact tends to be largest during late winter and early spring.

Overall, the analysis of precursor patterns and related timescales contributes to the understanding of the stratospheric pathway for Arctic-midlatitude linkages. Moreover, it helps to quantify which future changes in tropospheric pressure patterns (e.g. caused by AA) may lead to disruptions in the SPV. Additionally, White *et al* (2019) stated that tropospheric wave activity is larger preceding downward-propagating SSWs

**Figure 9.** Schematic for the life cycle of the stratosphere–troposphere oscillation (STO) (Shen *et al* 2023) and how other studies fit into the STO concept. For the schematic of STO, blue and red contours indicate cyclonic and anticyclonic anomalies. Purple arrows denote the propagation of Rossby waves. Orange arrows and black wavy arrows represent the effect of linear and nonlinear processes that account for the propagation of tropospheric circulation features. Text bubbles describe different types of research topics. Adapted with permission from Shen *et al* (2023). © American Meteorological Society. Used with permission.

compared with non-downward propagating events. This highlights the importance of precursor mechanisms. Köhler *et al* (2023) demonstrated the atmospheric model ICON is capable of realistically reproducing these mechanisms of troposphere–stratosphere coupling. An analysis of the precursor patterns and coupling mechanisms in the CMIP6 models would be of interest and could contribute to a better understanding of the large inter-model spread in the response of the strength of the SPV to future emission scenarios (e.g. Karpechko *et al* 2022).

### 4.5. Stratosphere–troposphere coupling on the intraseasonal timescale

Although the NAM has been known as the leading mode of SPV variation, it dominates only on timescales longer than 60 d (Shen *et al* 2023). In contrast, on the 10–60 d timescale, observations suggest that the zonal asymmetric mode, i.e. an SPV displacement, dominates over other variations of SPV (Shen *et al* 2023). This mode couples efficiently with the tropospheric circulation, forming a periodic oscillating phenomenon on the intraseasonal timescale, named the stratosphere–troposphere oscillation (STO; Shen *et al* 2023). Throughout its life cycle, the STO propagates westward periodically with a deep structure extending from the troposphere to the stratosphere (figure S10(c)). In the stratosphere, the STO is characterised by a wavenumber 1 structure, which propagates clockwise with time, reflecting the movement of the SPV towards North America, and then onwards to the North Pacific, Eurasia, and the North Atlantic (figure S10(a)). In the troposphere, the STO is manifested as a large-scale westward-propagating circulation in the midlatitudes, mainly located over the North Pacific (figure S10(b)).

The mechanism of the STO involves vertical and horizontal Rossby wave propagation (figures S10(c) and 9). The Rossby waves propagate upward from the troposphere into the stratosphere over East Asia, which maintains the STO's stratospheric component, then the reflection of these waves back to the troposphere contributes substantially to the development of the STO's tropospheric centre over North America. The vertical wave propagation presents a periodic change, alternating between upward and downward, and is inherent to changes in the STO's vertical structure, which are mainly attributed to the westward propagation of the tropospheric circulation. Meanwhile, linear processes and nonlinear cross-scale interactions explain the STO's westward propagation in the troposphere, which therefore facilitates changes in vertical wave propagation.

Strong and robust temperature changes over the mid-high latitudes are seen during the STO life cycle, where the temperature also shows an oscillation between cold and warm in accord with the circulation transition (figure S10(b)). This intraseasonal temperature anomaly can strongly contribute to the raw temperature change (Lin *et al* 2022) and, more importantly, it favours the occurrence of extreme temperature events (Guan *et al* 2020). For example, a strong cold extreme swept through North America in 2013/14 with features resembling the STO (Cohen *et al* 2022). From a statistical perspective, large-scale temperature extremes over North America are strongly linked with the shift of the SPV (Guan *et al* 2020, Cohen *et al* 2021). These sets of evidence together reinforce the role of STO in contributing to the extremes.

This newly defined STO phenomenon shares similarities with other studies on concepts of intraseasonal wintertime extratropical circulation in the NH. Early studies focusing on the troposphere found a clear westward retrograding circulation over the North Pacific (e.g. Takaya and Nakamura 2005). This retrograding mode is recognized as the dominant intraseasonal variation over this region, which presents a periodic phase change (Branstator 1987, Kushnir 1987), resembling the tropospheric circulation of STO. For the stratospheric component, the zonal asymmetric change of SPV, similar to the location shift in STO, is responsible for severe cold extremes over North America (Kretschmer *et al* 2018, Matthias and Kretschmer 2020) and occurs mainly via the wave reflection process (Ding *et al* 2022). In terms of stratosphere–troposphere coupling, a Western Hemisphere teleconnection resembling the STO was found to precede the SPV shift (Tan and Bao 2020), whereas the opposite tropospheric circulation is seen following the shift of SPV (Messori *et al* 2022). In addition, the wave-coupling is shown to occur on the intraseasonal timescale (Shaw *et al* 2014). Although those studies arose from different scientific questions, their results fit well into different parts of the STO concept.

Therefore, the STO unifies previous studies into one stratosphere–troposphere coupling framework, providing an holistic perspective to understand the wintertime extratropical atmospheric circulation. It not only offers potential for subseasonal-to-seasonal forecasting given its oscillating nature, but also provides new insight into understanding cold extremes over NH mid-high latitudes.
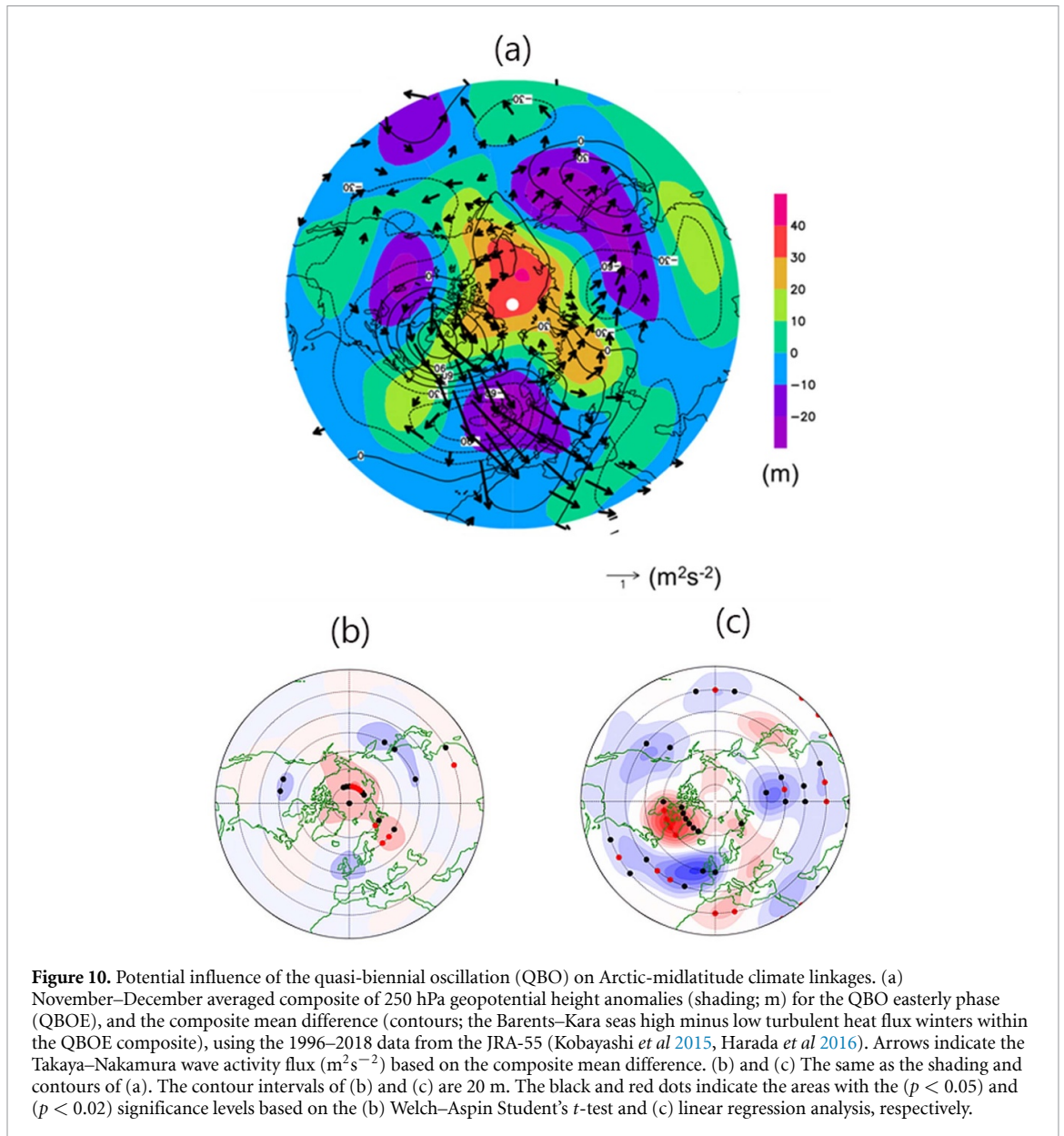
## 5. Role of the tropics in Arctic-midlatitude climate linkages

The QBO, Madden–Julian Oscillation (MJO) and ENSO are well-known modes of tropical atmosphere and oceanic variability that may have teleconnections with NH climate (e.g. Henderson *et al* 2014, Ye *et al* 2018, Ye and Jung 2019, Clancy *et al* 2021, Ma *et al* 2022). Equatorial/midlatitude connections relate to the increased upward arm of the Hadley cell that in turn can influence the latitudes of the Ferrel and Polar cell transition locations (Qian *et al* 2016a, 2016b). It is worth noting that each of those tropical modes of variability not only exert strong influence on the mid-latitude climate individually but can also interact with each other to modulate the eventual response. For example, ENSO is shown to modulate the influence of MJO on the polar vortex (e.g. Ma *et al* 2020), thereby affecting the mid-latitude climate response. In addition, the combined influence of QBO and ENSO on the stratosphere shows strong nonlinearity, yielding different atmospheric circulation responses in mid-latitudes (e.g. Walsh *et al* 2022, Ma *et al* 2023). This interaction shows that caution is needed when investigating the role of tropical variability in impacting Arctic-midlatitude climate linkages and CAO.

### 5.1. QBO
The QBO, which consists of alternating easterly (QBOE) and westerly (QBOW) zonal winds in the equatorial stratosphere at an average interval of 28 months, is driven by wave mean-flow interactions, namely the dissipation of wave-momentum fluxes arising from a range of tropospheric waves (Pahlavan *et al* 2021a, b, Anstey *et al* 2022). The QBO influences extra-tropical circulation in both the troposphere and stratosphere. The SPV is weaker during QBOE winters than during QBOW winters, known as the Holton–Tan relationship (e.g. Lu *et al* 2014; see figure S11), which is mainly explained by a shift of the zero-wind (critical) line that affects the propagation of planetary waves into the stratosphere.

The QBO also influences tropospheric circulation by modifying the vertical temperature profile of the tropics from the QBO-induced meridional circulation (Haynes *et al* 2021). During the QBOE phase, the tropical tropopause-layer temperature over the tropical Pacific warm pool region becomes lower by 1 °C–2 °C. This is linked to more active tropical convection and enhanced teleconnections into mid-to-high latitudes. Based on both observational and numerical results, Yamazaki *et al* (2020) showed the relevance of this process for the Holton–Tan relationship in the late-fall to early-winter period. Labe *et al* (2019) found that the early-winter upper tropospheric mean response to future Arctic sea-ice retreat is stronger during QBOE.

**Figure 10.** Potential influence of the quasi-biennial oscillation (QBO) on Arctic-midlatitude climate linkages. (a) November–December averaged composite of 250 hPa geopotential height anomalies (shading; m) for the QBO easterly phase (QBOE), and the composite mean difference (contours; the Barents–Kara seas high minus low turbulent heat flux winters within the QBOE composite), using the 1996–2018 data from the JRA-55 (Kobayashi *et al* 2015, Harada *et al* 2016). Arrows indicate the Takaya–Nakamura wave activity flux ($m^2s^{-2}$) based on the composite mean difference. (b) and (c) The same as the shading and contours of (a). The contour intervals of (b) and (c) are 20 m. The black and red dots indicate the areas with the ($p < 0.05$) and ($p < 0.02$) significance levels based on the (b) Welch–Aspin Student's *t*-test and (c) linear regression analysis, respectively.

The easterly phase of the QBO is associated with a weaker SPV and also with an enhanced upper-level circum-global height anomaly pattern with blocking highs in the early-winter period (colour shading on figure 10). The pattern includes a Ural high, which interacts constructively with the upper-level tropospheric height anomaly associated with sea-ice retreat in the BKS (solid contours in figure 10). This leads to an enhanced wave train over Eurasia that is often indicative of a severe Asian winter monsoon (arrows on figure 10). Zhang *et al* (2020) showed that during the QBOE, sea-ice loss over the Chukchi–Bering seas results in stronger upward wavenumber 2 propagation into the stratosphere, which affects the SSW with longer duration and stronger intensity followed by enhanced CAOs over the continents. Those results suggest that the QBO phase is a relevant factor for Arctic-midlatitude linkages by affecting the background circulation, which modulates the frequency of severe CAOs.

### 5.2. MJO

The MJO is the largest component of 30–90 d variability in the tropical atmosphere. It involves deep convection that slowly propagates eastwards above relatively warm parts of the Pacific and Indian Oceans (Zhang 2005) and is considered a remote source of predictability in the extratropics (Cassou 2008). An active MJO in certain phases influences large-scale flow in higher latitudes, such as the Euro-Atlantic
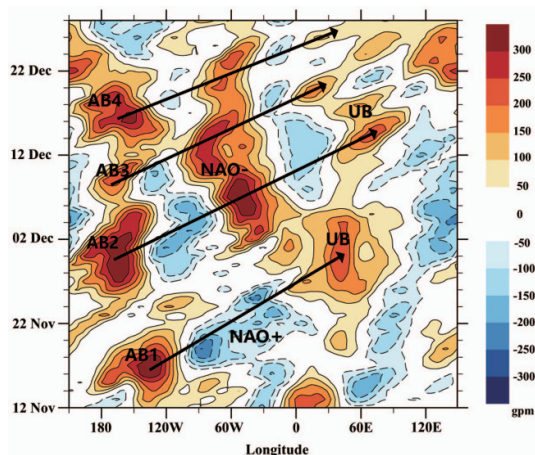
**Figure 11.** Rossby wave trains and interactions between the upstream and downstream atmospheric regimes provide important energy support for the maintenance of local atmospheric blocking episodes. Hovmöller diagram of the daily 500 hPa geopotential height anomalies (shading and contour, units: gpm) averaged over 40 °N–70 °N from 12 November–27 December 2022. AB1 to AB4 represent four consecutive Alaska blocking events, and UB is Ural blocking. Black lines with arrows indicate the propagation of Rossby wave packages. All the anomalies are calculated relative to the mean condition of 1979–2020. Adapted from Yao *et al* (2023), with permission from Springer Nature.

mid-tropospheric flow, and therefore favours CAOs (Ferranti *et al* 2018, Statnaia *et al* 2020, Knight *et al* 2021).

Figure S12 shows how the quality of CAO forecasts depends on MJO phase. We define predicted CAOs as the lower tercile of T2m in subseasonal-to-seasonal models at the extended-range timescales of weeks 3 and 4. The MJO is preferably in phases 6–8 during initialization of forecasts that correctly predicted CAOs for week 3 (figure S12(a)). Lin (2009) and Seo and Son (2012) showed that phases with the enhanced convection over the western and central Pacific excite wave trains that propagate poleward, which can influence extratropical flow patterns at a timescale of 2 weeks, favouring an onset of negative phase NAO. Forecasts with the MJO phase 3 in the initial conditions are responsible for the largest number of false alarm forecasts among all MJO phases. The MJO phase 3 often coincides with the Scandinavian Blocking regime in northern Europe that evolves into the positive phase NAO regime after approximately a week (Cassou 2008). The forecasts initiated during the MJO phase 3 and under the Scandinavian Blocking regime apparently take into account the persistence of the regime rather than the typical teleconnection from MJO. This results in the correct prediction of colder temperatures when the response from the MJO is not canonical (figures S12(b) and (c)). Given the considerable number of false-alarm forecasts following MJO phase 3, it suggests that forecasting systems give weight to the weather regime rather than relying on this remote precursor.

### 5.3. ENSO

Cooler sea-surface temperatures in the equatorial eastern Pacific Ocean (i.e. La Niña conditions) in conjunction with AA have been noted to weaken and shift the epicentre of UB or change the frequency of UB events and thus promote CAOs over China, Korea and Japan during early winter (Luo *et al* 2021). Against the backdrop of ongoing AA and the three-year La Niña during 2021–2023, the winter of 2022/23 was characterised by frequent and extreme CAOs in North America and Eurasia. Yao *et al* (2023) revealed the physical mechanism from the perspective of the potential vorticity gradient. Their study concluded that the meridional temperature gradient in the NH weakened owing to anomalous Arctic warming and tropical Pacific cooling, that led to a weakening of the meridional potential vorticity gradient at mid-high latitudes, which in turn favoured the frequent establishment and maintenance of NH high-latitude blocking. Therefore during the winter of 2022/23, the regimes within the Rossby wave trains were amplified. This enhancement can be attributed to the strengthened energy dispersion between the upstream and downstream atmospheric structure within the wavetrains, occurring against a weakened meridional potential vorticity gradients and significant downward propagation of stratospheric anomalies. Especially notable are the UB during the end of November and in mid-December and Alaska blocking around late December whose heightened persistence resulted in severe and disruptive CAOs (figure 11).

## 6. Recent insights using large-ensemble climate model simulations

Many of the disagreements in influences of AA could be caused by unclear causal relationships in observations and/or differing assumptions in modelling experiments, e.g. different forcings, resolutions, and model physics. To address these issues, the Polar Amplification Model Intercomparison Project (PAMIP) (Smith *et al* 2019, 2022) has coordinated an unprecedented set of multi-model ensemble experiments to understand the causes and consequences of AA induced by varying sea ice and sea-surface temperature. Results from the PAMIP multi-model ensemble suggest robust but weak influences of Arctic sea-ice loss on winter climate (Smith *et al* 2022). Some notable inter-model differences are noted such as the polar stratospheric response (Smith *et al* 2022). Further regional analyses revealed significant inter-model differences in the response of the North Atlantic polar jet to sea-ice loss (Ye *et al* 2023) (figure S13). A fundamental and outstanding question is does existing model ensemble size in single-model simulations or for individual models in the PAMIP quantify well the internal variability when assessing the response to AA? For any individual model in PAMIP and other modelling experiments, the ensemble size (typically between 100 and 500) may not be sufficiently large to fully separate forced response from internal variability (Peings *et al* 2021). The uncertainty in the forced response to projected Arctic sea-ice loss arising from internal variability has been extensively studied in recent very large-ensemble climate simulations (Ye *et al* 2024a). This could cause disagreements between modelling studies and confound inter-model comparisons. In particular, the response of extreme weather in midlatitudes to sea-ice loss is more challenging when dealing with relatively small GCM ensembles (e.g. Ye *et al* 2024b). Further uncertainty in how tropospheric circulation responds to Arctic sea-ice loss comes from stratospheric internal variability (Sun *et al* 2022).
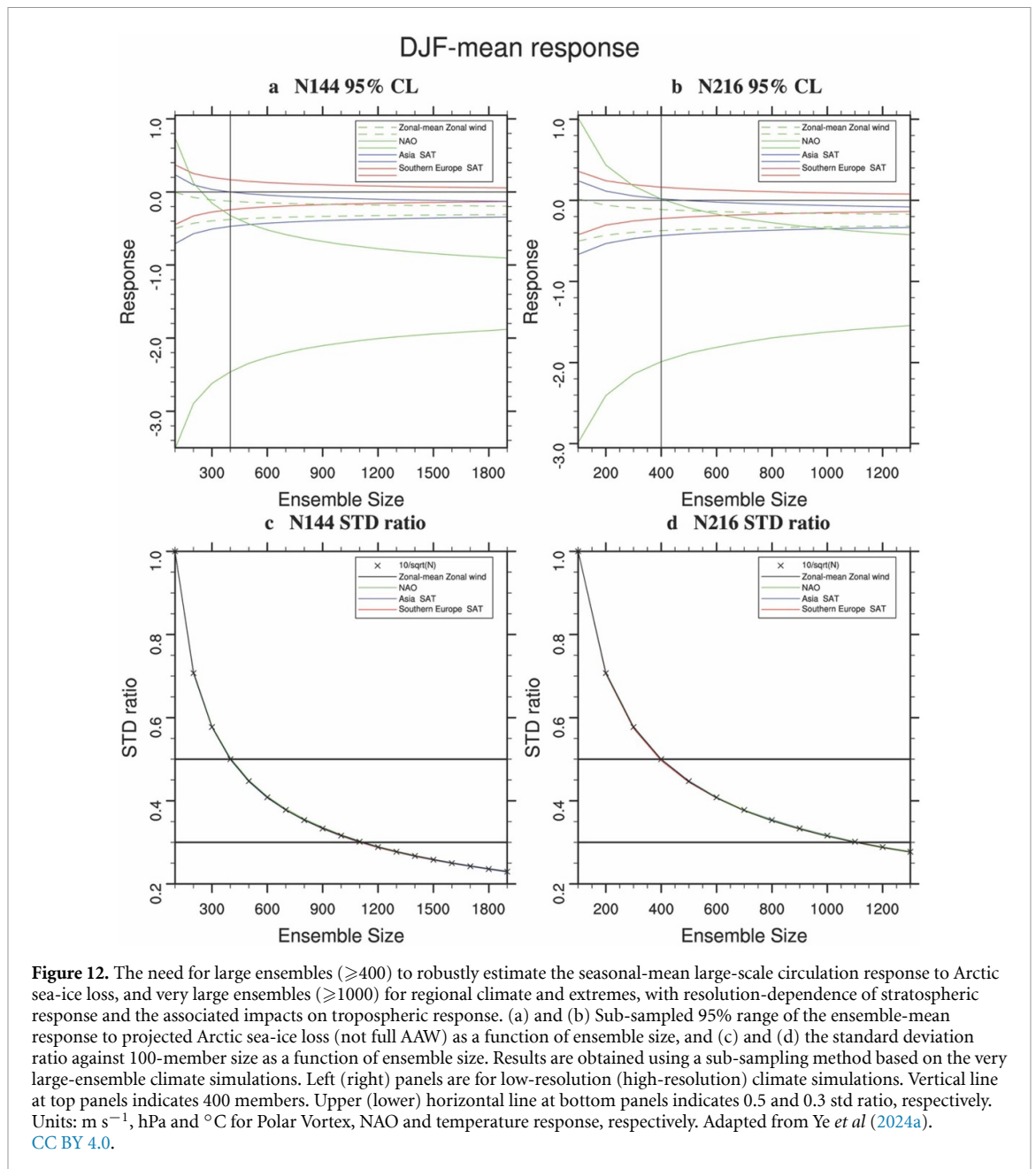
To address these issues and complement PAMIP, very large-ensemble, initial-condition climate model simulations have been conducted to understand the response of weather and climate to projected Arctic sea-ice loss under 2 °C global warming above pre-industrial levels (Ye *et al* 2024a). Analyses from these very large-ensemble climate simulations suggest that large ensembles (⩾400) are needed to robustly estimate the seasonal-mean large-scale circulation response, and very large ensembles (⩾1000) for regional climate and extreme weather events (figure 12). The analyses also identified resolution-dependence of the stratospheric response and the associated impacts on the troposphere (figure 12). The results suggest that previous modelling studies that show different response to Arctic sea-ice loss—such as different signs of NAO response—could be due to internal variability given their small ensemble size. It is noted that in the high-resolution simulations, even with very large-ensemble size, the stratospheric response to Arctic sea-ice loss is uncertain. This finding has implications for the role of the stratosphere in bridging AA effects on weather and climate variability.

One possible limitation is that the PAMIP simulations use sea-ice variability as the AA proxy. In the real world, both Arctic sea-ice loss and other forcings and feedbacks, such as temperature, contribute to Arctic atmospheric warming (e.g. Ye and Messori 2020), while Labe *et al* (2020) demonstrate that only considering sea-ice loss creates a much weaker forcing than total, more realistic AA. The PAMIP and Ye *et al* (2024a) studies likely underestimate the full impact of AA. There are currently no comparably extensive, targeted climate model experiments to study the full effects of AA other than fully-coupled simulations forced by differing scenarios of anthropogenic and natural factors.

## 7. Synthesis including future research priorities

Our research findings lead to important scientific and societal implications. The need is growing for early predictions of atmospheric circulation regimes likely to produce extreme weather across diverse socio-economic sectors that can significantly benefit from advanced warnings. An improved understanding of Arctic-midlatitude climate linkages benefits subseasonal-to-seasonal (S2S) weather predictions, covering outlooks for weeks up to 2 months, which are increasingly vital for weather-dependent planning (e.g. White *et al* 2021). Even if CAOs become less frequent and/or less intense overall, their impacts can be more significant as society under continued global warming becomes increasingly less prepared as CAOs penetrate into regions ill-equipped to respond. Given the potential high impact on large populations, further research is essential to improve understanding of climate-change-related teleconnections and their two-way interactions on the atmospheric dynamics responsible for the onset of CAOs. There is a need to look systematically and mechanistically at multiple cases of suspected Arctic/midlatitude weather connections, especially with the ongoing occurrence of extreme CAOs, such as during January 2024 in northern Europe (Rantanen *et al* 2024) and February 2021 in the south-central US.

The occurrence of extreme cold events is often caused by the synergy of multiple factors, including atmospheric modes such as a negative NAO pattern, high-latitude regional blocking over the Urals, Scandinavia, Greenland, and Alaska (Yao *et al* 2016, 2022, Zhuo *et al* 2022, Ballinger *et al* 2022, Ye and

**Figure 12.** The need for large ensembles (⩾400) to robustly estimate the seasonal-mean large-scale circulation response to Arctic sea-ice loss, and very large ensembles (⩾1000) for regional climate and extremes, with resolution-dependence of stratospheric response and the associated impacts on tropospheric response. (a) and (b) Sub-sampled 95% range of the ensemble-mean response to projected Arctic sea-ice loss (not full AAW) as a function of ensemble size, and (c) and (d) the standard deviation ratio against 100-member size as a function of ensemble size. Results are obtained using a sub-sampling method based on the very large-ensemble climate simulations. Left (right) panels are for low-resolution (high-resolution) climate simulations. Vertical line at top panels indicates 400 members. Upper (lower) horizontal line at bottom panels indicates 0.5 and 0.3 std ratio, respectively. Units: m s$^{-1}$, hPa and °C for Polar Vortex, NAO and temperature response, respectively. Adapted from Ye *et al* (2024a). CC BY 4.0.

Messori 2020, Tachibana *et al* 2019), and external forcing such as anomalies in sea ice, snow cover and sea-surface temperature in newly sea-ice free regions northwest of Alaska and the Barents Sea (Yao *et al* 2023, Zhang *et al* 2018a, Cohen *et al* 2012). The nature of the synergy between atmospheric modes is highly variable. Tracking changing trends of such synergies and identifying their commonalities is an important path and perspective for understanding the past and future CAOs. Mining the extended-range predictors of extreme cold events provides a useful tool for forecasting. For example, Song *et al* (2023) found that sea-ice anomalies in key regions during autumn play a role in regulating the frequency and intensity of UB and associated cold extremes in the following winter via changes in the winter tropospheric PVy due to weakened SPV. We advocate detailed research on dynamics and physical mechanisms of cold extremes and their predictors.

The frequent presence of hemispheric asymmetries in the structure of SPV (Cohen and Jones 2011), as well as the need to identify SPV disruptions that isolates stratospheric behaviour from the tropospheric influences, calls for defining a different metric to understand SPV disruptions and predict their influence on the mid-latitude weather. Here we propose a metric based on daily 50–10 hPa thickness anomaly fields during JF winter. This simple-to-calculate metric provides insight into SPV, as opposed to the traditional baroclinic stacking of height anomalies at 500 and 100 hPa (Cohen *et al* 2021). It removes tropospheric influences and reveals stratospheric dynamics that otherwise remain obscured by the lower atmosphere.

The PVy theory of the NMI blocking model provides a perspective on Arctic-midlatitude weather linkages, and as such can be used to identify their (potential) causal relationship. It addresses the questions of location, mechanism and duration. This theory can also be used to differentiate the various contributions of Arctic warming, ENSO, SPV disruptions (Chen *et al* 2021b, Song *et al* 2023), Pacific Decadal Oscillation, Atlantic Multidecadal Variability oceanic heatwaves, the 'cold pool' south of Greenland, and other background factors to winter cold extremes, summer heatwaves, Greenland Ice Sheet melting (Hanna *et al* 2009, 2014, Fettweis *et al* 2013, Wang and Luo 2022), and wildland fires (Jones *et al* 2022, Luo *et al* 2024). This PVy theory allows inference that long-lasting, intense and widespread winter cold extremes and summer heatwaves will be more frequent due to the presence of more persistent blocking events with larger zonal scale if PVy remains weaker under future global warming or Arctic warming in winter or summer. For example, rapid Arctic warming can increase the persistence of North American circulation patterns (Francis *et al* 2018) and summer sea-ice loss can enhance the risks of western North American wildfires (Zou *et al* 2021) and eastern Siberian wildfires (Luo *et al* 2024) via increasing the persistence of Siberian blocking due to reduced PVy. Weakening of the winter SPV can lead to a reduced PVy along Northern Hemispheric midlatitudes in the troposphere (Chen *et al* 2021b), thus promoting CAOs over continents via increasing the persistence and zonal scale of blocking events. However, the temperature extremes will be suppressed if PVy is below a critical threshold under future Arctic warming.

Research should investigate the relative importance of both large- and synoptic-scale drivers and local factors (orography, snow/ice cover, clouds, surface energy budget, ABL structure) that determine the local severity of extreme CAOs. This can be done by applying the methodology that Nygård *et al* (2023) used for temperature data from the 850 hPa level to near-surface (2 m) temperatures. Differences in the results between the two levels would give insight to the role of surface forcing and ABL processes. Such an approach is motivated by differences in the conclusions of Sui *et al* (2020) and Nygård *et al* (2023), based on differing temperature data: 2 m air temperatures were used in the former study, indicating decreased occurrence of wintertime cold extremes in northern Europe, whereas 850 hPa temperatures were used in the latter, only indicating minor changes in the strength and occurrence in Europe.

We highlight important types of stratosphere–troposphere coupling via SPV location changes and stretching, which has been understudied relative to the previous primary focus on SSWs, even though the impact of the former SPV events on North American temperatures can be of greater extent, magnitude, and frequency (Kretschmer *et al* 2018). A key priority is therefore identifying and understanding the shape and movement of the SPV over continents, considering the vertical coherence between 100 mb and 500 mb geopotential height features, and surface weather (Cohen *et al* 2021, Overland *et al* 2021). Improved understanding of the patterns and processes of vortex behaviour can extend the lead time for warning of cold extremes in Eurasia, the eastern US and Canada. Future research should aim to explain the connection between AA, SPV events, and their influence on severe winter weather in North America and Eurasia. Furthermore, the characterisation of the SPV before and after a SSW event could provide useful information in improving weather predictability, especially over North America, although more in-depth analysis is needed to understand how the vortex types influence the tropospheric circulation and thus surface weather. The reasons why some SSWs are not associated with the characteristic surface impacts needs to be better understood. It is important to quantify and characterize inter-event variability, and how this may change under future climate scenarios. Improved prediction of surface impacts associated with individual SPV events and CAOs is crucial for mitigating their effects on society.

The stratosphere–troposphere coupled oscillation that we report should be further investigated, including its dynamic mechanism, long-term trend and capability of model simulations. Regarding its dynamics, the diversity of the STO should be analysed, including its life cycle and the tropospheric response. While studies have reported that some CMIP6 models can capture the wave reflection process and subsequent tropospheric response similar to STO (Ding *et al* 2023a, 2023b), it is important to systematically study whether GCMs can reproduce the entire oscillation. Understanding of the STO offers an additional perspective for S2S forecast skill. Given that STO strongly influences surface temperature, and the fact that CAOs still occur despite global warming, it is worthwhile to investigate the STO.

A more holistic physical explanation of the coupling process between the northern SPV and high-latitude blocking at intra-seasonal timescales, with additional forcing from surface conditions by snow and sea ice, is required. There is a clear opportunity for further research to address the combination of these factors.

There is some evidence for tropical modulation of Arctic-midlatitude climate linkages through teleconnections associated with the QBO, MJO and ENSO. Regarding possible QBO forcing, although the enhanced upper-level circumpolar height anomaly pattern with blocking highs in early winter (section 5.1) is observationally a robust signature, a better understanding of its relationship with tropical convection is required. MJO phase through enhanced convection over the tropical Pacific seems to be able to influence airflow, blocking and CAO over Europe (section 5.2). La Niña-related eastern tropical Pacific sea-surface

**Figure 13.** Overview schematic of Arctic-midlatitude weather/climate linkages in a stratospheric polar vortex and high-latitude blocking context, adapted from Kretschmer *et al* (2020). CC BY 4.0. Key high-latitude blocking features shown are Alaska blocking (AB), Greenland blocking (GB), Scandinavian blocking (SB), and Ural blocking/sea-level pressure (Ural-SLP). Also shown is North Pacific sea-level pressure. Two sea-ice regions are depicted: North Pacific sea-ice concentration and Barents–Kara seas sea-ice concentration. v'T' denotes eddy heat flux. Potential tropical drivers of Arctic-midlatitude linkages are shown: El Niño Southern Oscillation, Madden–Julian Oscillation and the quasi-biennial oscillation. The striped box indicates the high-latitude region of interest where blocking occurrence is affected by changes in the meridional gradient of potential vorticity (PVy), which in turn is affected by Arctic amplification and sometimes mid-latitude cooling. Adapted from Kretschmer *et al* (2020). CC BY 4.0.

temperature cooling in combination with AA together with the excitation of Rossby waves from the tropics in this ENSO phase favours the development of northern high-latitude blocking and therefore CAOs. Although the time scales of the MJO, QBO, and ENSO range from weeks to years, there is evidence that they are interrelated, e.g. a larger MJO amplitude and more active convection in the Pacific warm pool region, i.e. La Niña condition, during the QBOE regime. This calls for future research to be directed towards a better understanding of an integrated tropical modulating role on AA/midlatitude linkage.

Sweeney *et al* (2024) show that internal variability from 1979–2022 has enhanced Arctic warming but cooled other regions (e.g. tropical eastern Pacific), resulting in a smaller meridional temperature gradient and thus a weaker PVy. It is an important future research task to separate that part of the global warming due to anthropogenic forcings from that due to natural variability. We present an overview schematic of Arctic-midlatitude weather/climate linkages, based on the potential drivers and interactions discussed above, focusing on high-latitude blocking, PVy, SPV and possible connections to the tropics (figure 13). This shows interconnections between all the different climate processes and drivers reviewed above.

Large-ensemble GCM studies are an essential tool to complement evidence from observations. Future research could be carried out to take full advantage of the sheer ensemble size by the very large-ensemble climate simulations and PAMIP model output, and to complement these large ensembles using large-ensemble fully-coupled models with well-resolved stratospheres. Key priorities include further quantifying internal variability in the response to Arctic sea-ice loss in coupled model simulations, and more detailed investigations of the role of the stratosphere in bridging the influence of Arctic sea-ice loss and AA. However, greater recognition of the need to include the full effects of AA (beyond just sea-ice loss) and a

good representation of the stratosphere in such large-ensemble GCM simulations are also required to obtain realistic responses of extreme winter weather regimes to a rapidly warming Arctic.

In this review we have shown how Arctic-midlatitude climate linkages are influenced by nonlinear blocking and by different modes of SPV variability, moving beyond the current predominant focus on SSWs. Such linkages are preconditioned by multiple tropical sources (ENSO, MJO, QBO) and require very large climate model ensembles to be properly understood. Enhanced studies of blocking, SPV, their vertical coupling, connections to CAOs and their resulting impacts, and more diverse and comprehensive model results based on newly-available large-ensemble projections, form important ways forward for conceptual understanding of Arctic-midlatitude climate linkages in the era of global warming and AA and for advancing synoptic to seasonal weather forecasting.

## Data availability statement

The data that support the findings of this study are available upon reasonable request from the authors.

## Acknowledgment

## Author contributions

EH coordinated the study and led the writing, together with a core group consisting of J F, M W, J E O, J C, D L, and T V. All authors contributed to the writing and discussion of ideas.

## Open data and code

Figures 6, S3 and S4 were produced using the Interactive Data Language (IDL), and the Climate Data Operator (CDO) software was also used for manipulating and analysing climate data (Bowman 2006, Schulzweida 2019). Figures 10 and S11 were produced using the Grid Analysis and Display System (GrADS) and the Climate Data Operator (CDO) software and the Python language. Codes utilized in this study can be provided upon request.

## ORCID iDs

Edward Hanna ⬤ https://orcid.org/0000-0002-8683-182X
Jennifer Francis ⬤ https://orcid.org/0000-0002-7358-9296
Muyin Wang ⬤ https://orcid.org/0000-0001-5233-4588

James E Overland ⓘ https://orcid.org/0000-0002-2012-8832
Judah Cohen ⓘ https://orcid.org/0000-0002-7762-4482
Dehai Luo ⓘ https://orcid.org/0000-0001-8834-8623
Timo Vihma ⓘ https://orcid.org/0000-0002-6557-7084
Qiang Fu ⓘ https://orcid.org/0000-0001-5371-8460
Richard J Hall ⓘ https://orcid.org/0000-0003-4840-383X
Ralf Jaiser ⓘ https://orcid.org/0000-0002-5685-9637
Seong-Joong Kim ⓘ https://orcid.org/0000-0002-6232-8082
Raphael Köhler ⓘ https://orcid.org/0000-0002-3378-8012
Linh Luu ⓘ https://orcid.org/0000-0003-0659-9248
Xiaocen Shen ⓘ https://orcid.org/0009-0003-7116-1397
Irene Erner ⓘ https://orcid.org/0000-0003-3066-1902
Jinro Ukita ⓘ https://orcid.org/0000-0001-6461-179X
Yao Yao ⓘ https://orcid.org/0000-0002-6425-7855
Kunhui Ye ⓘ https://orcid.org/0000-0002-9433-8066
Hyesun Choi ⓘ https://orcid.org/0000-0002-9298-9148
Natasa Skific ⓘ https://orcid.org/0000-0002-7239-8981

## Reference

Afargan-Gerstman H and Domeisen D I V 2020 Pacific modulation of the North Atlantic storm track response to sudden stratospheric warming events *Geophys. Res. Lett.* **47** e2019GL085007
AMS 2019 polar vortex *Glossary of Meteorology* (American Meteorological Society) (available at: glossary.ametsoc.org/wiki/Polar_vortex)
Anstey J A, Osprey S M, Alexander J, Baldwin M P, Butchart N, Gray L, Kawatani Y, Newman P and Richter J H 2022 Impacts, processes and projections of the quasi-biennial oscillation *Nat. Rev. Earth Environ.* **3** 588–603
Armour K C, Bitz C M and Roe G H 2013 Time-varying climate sensitivity from regional feedback *J. Clim.* **26** 4518–34
Ashley W S, Haberlie A M and Gensini V A 2020 Reduced frequency and size of late-twenty-first-century snowstorms over North America *Nat. Clim. Change* **10** 539–44
Ayarzaguena B *et al* 2020 Uncertainty in the response of sudden stratospheric warmings and stratosphere-troposphere coupling to quadrupled $CO_2$ concentrations in CMIP6 models *J. Geophys. Res. Atmos.* **125** e2019JD032345
Bailey H, Hubbard A, Klein E S, Mustonen K R, Akers P D, Marttila H and Welker J M 2021 Arctic sea-ice loss fuels extreme European snowfall *Nat. Geosci.* **14** 283–8
Baldwin M P *et al* 2021 Sudden stratospheric warmings *Rev. Geophys.* **59** e2020RG000708
Baldwin M P and Dunkerton T J 1999 Propagation of the Arctic Oscillation from the stratosphere to the troposphere *J. Geophys. Res. Atmos.* **104** 30937–46
Baldwin M P and Dunkerton T J 2001 Stratospheric Harbingers of Anomalous Weather Regimes *Science* **294** 581–4
Ballinger T J *et al* 2023 Surface air temperature *Arctic Report Card 2023* (National Oceanographic and Atmospheric Administration, NOAA) (available at: arctic.noaa.gov/report-card/report-card-2023/surface-air-temperature-2023/)
Ballinger T J, Walsh J E, Alexeev V A, Bieniek P A and McLeod J T 2022 The Alaska Blocking Index, version 2: analysis and covariability with statewide and large-scale climate from 1948 to 2020 *Int. J. Climatol.* **42** 9767–87
Barlow M 2024 Extreme cold still happens in a warming world—in fact climate instability may be disrupting the polar vortex (theconversation.com) (available at: https://theconversation.com/extreme-cold-still-happens-in-a-warming-world-in-fact-climate-instability-may-be-disrupting-the-polar-vortex-221276)
Black R X and McDaniel B A 2004 Diagnostic case studies of the Northern Annular Mode *J. Clim.* **17** 3990–4004
Blackport R, Fyfe J C and Screen J A 2022 Arctic change reduces risk of cold extremes *Science* **375** 729
Blackport R and Screen J A 2020 Weakened evidence for midlatitude impacts of Arctic warming *Nat. Clim. Change* **10** 1065–6
Blackport R, Screen J A, van der Wiel K and Bintanja R 2019 Minimal influence of reduced Arctic sea ice on coincident cold winters in midlatitudes *Nat. Clim. Change* **9** 697–704
Bowman K P 2006 *An Introduction to Programming with IDL: Interactive Data Language* (Academic Press)
Branstator G 1987 A striking example of the atmosphere's leading traveling pattern *J. Atmos. Sci.* **44** 2310–23
Bretones A, Nisancioglu K H, Jensen M F, Brakstad A and Yang S 2022 Transient increase in Arctic deep-water formation and ocean circulation under sea ice retreat *J. Clim.* **35** 109–24
Butchart N 2022 The stratosphere: a review of the dynamics and variability *Weather Clim. Dyn.* **3** 1237–72
Butler A H, Lawrence Z D, Lee S H, Lillo S P and Long C S 2020 Differences between the 2018 and 2019 stratospheric polar vortex split events *Q. J. R. Meteorol. Soc.* **146** 3503–21
Cai D, Lohmann G, Chen X and Ionita M 2024 The linkage between autumn Barents–Kara sea ice and European cold winter extremes *Front. Clim.* **6** 1345763
Cassou C 2008 Intraseasonal interaction between the Madden–Julian Oscillation and the North Atlantic Oscillation *Nature* **455** 523–7
Charlton A J and Polvani L M 2007 A new look at stratospheric sudden warmings. Part I: Climatology and modelling benchmarks *J. Clim.* **20** 449–69
Chen S, Yu B, Wu R, Chen W and Song L 2021c The dominant North Pacific atmospheric circulation patterns and their relations to Pacific SSTs: historical simulations and future projections in the IPCC AR6 models *Clim. Dyn.* **56** 701–25
Chen X, Dai A, Wen Z and Song Y 2021a Contributions of Arctic sea-ice loss and East Siberian atmospheric blocking to 2020 record-breaking Meiyu–Baiu rainfall *Geophys. Res. Lett.* **48** e2021GL092748
Chen X, Luo D, Wu Y, Dunn-Sigouin E and Lu J 2021b Nonlinear response of atmospheric blocking to early winter Barents–Kara seas warming: an idealised model study *J. Clim.* **34** 2367–83
Choi H, Kim B-M and Choi W 2019 Type classification of sudden stratospheric warming based on pre- and postwarming periods *J. Clim.* **32** 2349–67

Choi H, Kim J-H, Kim B-M and Kim S-J 2021 Observational evidence of distinguishable weather patterns for three types of sudden stratospheric warming during Northern winter *Front. Earth Sci.* **9** 625868

Clancy R, Bitz C and Blanchard-Wrigglesworth E 2021 The influence of ENSO on Arctic sea ice in large ensembles and observations *J. Clim.* **34** 9585–604

Cohen J L, Furtado J C, Barlow M A, Alexeev V A and Cherry J E 2012 Arctic warming, increasing snow cover and widespread boreal winter cooling *Environ. Res. Lett.* **7** 014007

Cohen J *et al* 2014 Recent Arctic amplification and extreme midlatitude weather *Nat. Geosci.* **7** 627–37

Cohen J *et al* 2020 Divergent consensus on Arctic amplification influence on midlatitude severe winter weather *Nat. Clim. Change* **10** 20–29

Cohen J, Agel L, Barlow M and Entekhabi D 2023 No detectable trend in midlatitude cold extremes during the recent period of Arctic amplification *Commun. Earth Environ.* **4** 341

Cohen J, Agel L, Barlow M, Furtado J C, Kretschmer M and Wendt V 2022 The 'polar vortex' winter of 2013/2014 *J. Geophys. Res. Atmos.* **127** e2022JD036493

Cohen J, Agel L, Barlow M, Garfinkel C I and White I 2021 Linking Arctic variability and change with extreme winter weather in the United States *Science* **373** 1116–21

Cohen J and Jones J 2011 Tropospheric precursors and stratospheric warmings *J. Clim.* **24** 6562–72

Cohen J, Pfeiffer K and Francis J A 2018 Warm Arctic episodes linked with increased frequency of extreme winter weather in the United States *Nat. Commun.* **9** 869

Coumou D and Rahmstorf S 2012 A decade of weather extremes *Nat. Clim. Change* **2** 491–6

Coumou S, Lehmann J and Beckmann J 2015 The weakening summer circulation in the Northern Hemisphere midlatitudes *Science* **17** 324–7

Dai A G and Song M R 2020 Little influence of Arctic amplification on midlatitude climate *Nat. Clim. Change* **10** 231–7

Dai A, Luo D, Song M and Liu J 2019 Arctic amplification is caused by sea-ice loss under increasing $CO_2$ *Nat. Commun.* **10** 121

Davy R, Esau I, Chernokulsky A, Outten S and Zilitinkevich S 2017 Diurnal asymmetry to the observed global warming *Int. J. Climatol.* **37** 79–93

Dee D P *et al* 2011 The ERA-Interim reanalysis: configuration and performance of the data assimilation system *Q. J. R. Meteorol. Soc.* **137** 553–97

Delhasse A, Hanna E, Kittel C and Fettweis X 2021 Brief communication: CMIP6 does not suggest any atmospheric blocking increase in summer over Greenland by 2100 *Int. J. Climatol.* **41** 2589–96

Ding Q, Wallace J M, Battisti D S, Steig E J, Gallant A J E, Kim H-J and Geng L 2014 Tropical forcing of the recent rapid Arctic warming in northeastern Canada and Greenland *Nature* **509** 209–12

Ding T, Gao H and Li X 2021 Increasing occurrence of extreme cold surges in North China during the recent global warming slowdown and the possible linkage to the extreme pressure rises over Siberia *Atmos. Res.* **248** 105198

Ding X, Chen G and Ma W 2023a Stratosphere-troposphere coupling of extreme stratospheric wave activity in CMIP6 models *J. Geophys. Res.* **128** e2023JD038811

Ding X, Chen G, Sun L and Zhang P 2022 Distinct North American cooling signatures following the zonally symmetric and asymmetric modes of winter stratospheric variability *Geophys. Res. Lett.* **49** e2021GL096076

Ding X, Chen G, Zhang P, Domeisen D I V and Orbe C 2023b Extreme stratospheric wave activity as harbingers of cold events over North America *Commun. Earth Environ.* **4** 187

Dixon P G, Brommer D M, Hedquist B C, Kalkstein A J, Goodrich G B, Walter J C, Dickerson IV C C, Penny S J and Cerveny R S 2005 Heat mortality versus cold mortality: a study of conflicting databases in the United States *Bull. Am. Meteorol. Soc.* **86** 937–44

Domeisen D I V 2019 Estimating the frequency of sudden stratospheric warming events from surface observations of the North Atlantic Oscillation *J. Geophys. Res. Atmos.* **124** 3180–94

Domeisen D I V *et al* 2020 The role of the stratosphere in subseasonal to seasonal prediction Part II: predictability arising from stratosphere - troposphere coupling *J. Geophys. Res. Atmos.* **125** e2019JD030923

DW.com 2021 German village logs −28.9 Celsius as cold snap persists (available at: www.dw.com/en/german-village-logs-289-celsius-overnight-as-cold-snap-persists/a-56576765)

Eichmann M 2024 *Freezer Scandinavia* (MeteoNews) (Accessed 4 January 2024)

Elsbury D, Peings Y and Magnusdottir G 2021 CMIP6 models underestimate the Holton–Tan effect *Geophys. Res. Lett.* **48** e2021GL094083

England M R, Eisenman I, Lutsko N J and Wagner T J W 2021 The recent emergence of Arctic amplification *Geophys. Res. Lett.* **48** e2021GL094086

Erner I and Karpechko A 2024 Factors influencing subseasonal predictability of northern Eurasian cold spells *Q. J. R. Meteorol. Soc* **150** 2955–75

Euronews.com 2021 Spain records coldest ever temperature at −35.8 °C (available at: www.euronews.com/2021/01/07/spain-records-coldest-ever-temperature-at-35-8-c)

Ferranti L, Magnusson L, Vitart F and Richardson D S 2018 How far in advance can we predict changes in large-scale flow leading to severe cold conditions over Europe? *Q. J. R. Meteorol. Soc.* **144** 1788–802

Fettweis X, Hanna E, Lang C, Belleflamme A, Erpicum M and Gallée H 2013 Brief communication: important role of the mid-tropospheric atmospheric circulation in the recent surface melt increase over the Greenland ice sheet *Cryosphere* **7** 241–8

Field C B (eds) *et al* 2012 *Managing the Risks of Extreme Events and Disasters to Advance Climate Change Adaptation. A Special Report of the Intergovernmental Panel on Climate Change* (IPCC)

Francis J A 2015 The Arctic matters: extreme weather responds to diminished Arctic Sea ice *Environ. Res. Lett.* **10** 091002

Francis J A, Skific N and Vavrus S J 2018 North American weather regimes are becoming more persistent: is Arctic amplification a factor? *Geophys. Res. Lett.* **45** 11–414

Francis J A and Vavrus S J 2012 Evidence linking Arctic amplification to extreme weather in midlatitudes *Geophys. Res. Lett.* **39** L06801

Francis J A and Vavrus S J 2015 Evidence for a wavier jet stream in response to rapid Arctic warming *Environ. Res. Lett.* **10** 014005

Fyfe J C 2019 Midlatitudes unaffected by sea ice loss *Nat. Clim. Change* **9** 648–52

Gan B, Wu L, Jia F, Li S, Cai W, Nakamura H, Alexander M A and Miller A J 2017 On the Response of the Aleutian low to greenhouse warming *J. Clim.* **30** 3907–25

Garfinkel C I and Hartmann D L 2008 Different ENSO teleconnections and their effects on the stratospheric polar vortex *J. Geophys. Res.* **113**

Garfinkel C I, Hartmann D L and Sassi F 2010 Tropospheric precursors of anomalous Northern Hemisphere stratospheric polar vortices *J. Clim.* **23** 3282–99

Giamalaki K, Beaulieu C, Henson S A, Martin A P, Kassem H and Faranda D 2021 Future intensification of extreme Aleutian low events and their climate impacts *Sci. Rep.* **11** 18395

Graversen R G and Burtu M 2016 Arctic amplification enhanced by latent energy transport of atmospheric planetary waves *Q. J. R. Meteorol. Soc.* **142** 2046–54

Graversen R G and Wang M 2009 Polar amplification in a coupled climate model with locked albedo *Clim. Dyn.* **33** 629–43

Guan W, Jiang X, Ren X, Chen G, Lin P and Lin H 2020 The leading intraseasonal variability mode of wintertime surface air temperature over the North American sector *J. Clim.* **33** 9287–306

Hahn L C, Armour K C, Zelinka M D, Bitz C M and Donohoe A 2021 Contributions to polar amplification in CMIP5 and CMIP6 models *Front. Earth Sci.* 710036 **9**

Hall R J, Hanna E and Chen L 2021 Winter Arctic amplification at the synoptic timescale, 1979–2018, its regional variation and response to tropical and extratropical variability *Clim. Dyn.* **56** 457–73

Hall R J, Mitchell D M, Seviour W J M and Wright C J 2022 How well are sudden stratospheric warming surface impacts captured by CMIP6 models? *J. Geophys. Res. Atmos.* **127** e2021JD035725

Hall R J, Mitchell D M, Seviour W J M and Wright C J 2023 Surface hazards in North-west Europe following sudden stratospheric warming events *Environ. Res. Lett.* **18** 064002

Hall R, Erdélyi R, Hanna E, Jones J M and Scaife A A 2015 Drivers of North Atlantic polar front jet stream variability *Int. J. Climatol.* **35** 1697–720

Hanna E, Cappelen J, Fettweis X, Huybrechts P, Luckman A and Ribergaard M H 2009 Hydrologic response of the Greenland ice sheet: the role of oceanographic warming *Hydrol. Proc.* **23** 7–30

Hanna E, Cropper T E, Hall R J and Cappelen J 2016 Greenland Blocking Index 1851–2015: a regional climate change signal *Int. J. Climatol.* **36** 4847–61

Hanna E, Cropper T E, Jones P D, Scaife A A and Allan R 2015 Recent seasonal asymmetric changes in the NAO (a marked summer decline and increased winter variability) and associated changes in the AO and Greenland Blocking Index *Int. J. Climatol.* **35** 2540–54

Hanna E, Fettweis X and Hall R J 2018 Brief communication: recent changes in summer Greenland blocking captured by none of the CMIP5 models *Cryosphere* **12** 3287–92

Hanna E, Fettweis X, Mernild S H, Cappelen J, Ribergaard M H, Shuman C A, Steffen K, Wood L and Mote T L 2014 Atmospheric and oceanic climate forcing of the exceptional Greenland ice sheet surface melt in summer 2012 *Int. J. Climatol.* **34** 1022–37

Harada Y, Kamahori H, Kobayashi C, Endo H, Kobayashi S, Ota Y, Onoda H, Onogi K, Miyaoka K and Takahashi K 2016 The JRA-55 Reanalysis: representation of atmospheric circulation and climate variability *J. Meteor. Soc. Japan* **94** 269–302

Haynes P, Hitchcock P, Hitchman M, Yoden S, Hendon H, Kiladis G, Kodera K and Simpson I 2021 The influence of the stratosphere on the tropical troposphere *J. Met. Soc. Japan* **99** 803–45

Henderson G R, Barrett B S and Lafleur D M 2014 Arctic sea ice and the Madden–Julian Oscillation (MJO) *Clim. Dyn.* **43** 2185–96

Henderson G R, Barrett B S, Wachowicz L J, Mattingly K S, Preecem J R and Mote T L 2021 Local and remote atmospheric circulation drivers of Arctic change: a review *Front. Earth Sci.* **9** 709896

Hersbach H *et al* 2020 The ERA5 global reanalysis *Q. J. R. Meteorol. Soc.* **146** 1999–2049

Honda M, Inoue J and Yamane S 2009 Influence of low Arctic sea-ice minima on anomalously cold Eurasian winters *Geophys. Res. Lett.* **36** L08707

Hong Y, S-y S W, Son S-W, Jeong J-H, Kim S-W, Kim B, Kim H and Yoon J-H 2024 From peak to plummet: impending decline of the warm Arctic-cold continents phenomenon *npj Clim. Atmos. Sci.* **7** 66

Hoshi K, Ukita J, Honda M, Nakamura T, Yamazaki K, Miyoshi Y and Jaiser R 2019 Weak stratospheric polar vortex events modulated by the Arctic sea-ice loss *J. Geophys. Res. Atmos.* **124** 858–69

Huang J, Hitchcock P, Maycock A C, McKenna C M and Tian W 2021 Northern hemisphere CAOs are more likely to be severe during weak polar vortex conditions *Commun. Earth Environ.* **2** 147

Jaiser R, Akperov M, Timazhev A, Romanowsky E, Handorf D and Mokhov I I 2023 Linkages between Arctic and midlatitude weather and climate: unraveling the impact of changing sea ice and sea surface temperatures *Meteorol. Z.* **32** 173–94

Jaiser R, Nakamura T, Handorf D, Dethloff K, Ukita J and Yamazaki K 2016 Atmospheric winter response to Arctic sea ice changes in reanalysis data and model simulations *J. Geophys. Res. Atmos.* **121** 7564–77

Jones M W *et al* 2022 Global and regional trends and drivers of fire under climate change *Rev. Geophys.* **60** e2020RG000726

Kalnay E *et al* 1996 The NCEP/NCAR 40-year reanalysis project *Bull. Am. Meteorol. Soc.* **77** 437–72

Karpechko A Y, Afargan-Gerstman H, Butler A H, Domeisen D I V, Kretschmer M, Lawrence Z, Manzini E, Sigmond M, Simpson I R and Wu Z 2022 Northern hemisphere stratosphere-troposphere circulation change in CMIP6 models: 1. Inter-model spread and scenario sensitivity *J. Geophys. Res. Atmos.* **127** e2022JD036992

Karpechko A Y, Hitchcock P, Pieters D H W and Schneidereit A 2017 Predictability of downward propagation of major sudden stratospheric warmings *Q. J. R. Meteorol. Soc.* **143** 1459–70

Kaufman Z, Feldl N and Beaulieu C 2024 Warm Arctic-cold Eurasia pattern driven by atmospheric blocking in models and observations *Environ. Res. Clim.* **3** 015006

Kautz L A, Polichtchouk I, Birner T, Garny H and Pinto J G 2020 Enhanced extended-range predictability of the 2018 late-winter Eurasian cold spell due to the stratosphere *Q. J. R. Meteorol. Soc.* **146** 1040–55

Kidston J, Scaife A A, Hardiman S C, Mitchell D M, Butchart N, Baldwin M P and Gray L J 2015 Stratospheric influence on tropospheric jet streams, storm tracks and surface weather *Nat. Geosci.* **8** 433–40

Kim B-M, Son S-W, Min S-K, Jeong J H, Kim S-J, Zhang X, Shim T and Yoon J-H 2014 Weakening of the stratospheric polar vortex by Arctic sea-ice loss *Nat. Commun.* **5** 4646

King A D, Butler A H, Jucker M, Earl N O and Rudeva I 2019 Observed relationships between sudden stratospheric warmings and European climate extremes *J. Geophys. Res. Atmos.* **124** 13943–61

Knight J *et al* 2021 Predictability of European winters 2017/2018 and 2018/2019: contrasting influences from the tropics and stratosphere *Atmos. Sci. Lett.* **22** e1009

Kobayashi S *et al* 2015 The JRA-55 Reanalysis: general specifications and basic characteristics *J. Meteor. Soc. Japan* **93** 5–48

Köhler R H, Jaiser R and Handorf D 2023 How do different pathways connect the stratospheric polar vortex to its tropospheric precursors? *Weather Clim. Dyn.* **4** 1071–86

Kolstad E W, Wulff C O, Domeisen D I V and Woollings T 2020 Tracing North Atlantic Oscillation forecast errors to stratospheric origins *J. Clim.* **33** 9145–57

Kretschmer M, Cohen J, Matthias V, Runge J and Coumou D 2018 The different stratospheric influences on cold extremes in northern Eurasia and North America *npj Clim. Atmos. Sci.* **1** 44

Kretschmer M, Zappa G and Shepherd T G 2020 The role of Barents–Kara sea ice loss in projected polar vortex changes *Weather Clim. Dyn.* **1** 715–30

Kug J-S, Jeong J H, Jang Y S, Kim B-M, Folland C K, Min S-K and Son S-W 2015 Two distinct influences of Arctic warming on cold winters over North America and East Asia *Nat. Geosci.* **8** 759–62

Kushnir Y 1987 Retrograding wintertime low-frequency disturbances over the North Pacific Ocean *J. Atmos. Sci.* **44** 2727–42

Labe Z, Peings Y and Magnusdottir G 2019 The effect of QBO phase on the atmospheric response to projected Arctic sea ice loss in early winter *Geophys. Res. Lett.* **46** 7663–71

Labe Z, Peings Y and Magnusdottir G 2020 Warm Arctic, cold Siberia pattern: role of full Arctic amplification versus sea ice loss alone *Geophys. Res. Lett.* **47** e2020GL088583

Laloyaux P, Balmaseda M, Dee D, Mogensen K and Janssen P 2016 A coupled data assimilation system for climate reanalysis *Q. J. R. Meteorol. Soc.* **142** 65–78

Lee J-Y *et al* 2021 Future global climate: scenario-based projections and near-term information *Climate Change 2021: The Physical Science Basis. Contribution of Working Group I to the Sixth Assessment Report of the Intergovernmental Panel on Climate Change* ed V Masson-Delmotte *et al* (Cambridge University Press) pp 553–672

Li M, Luo D, Simmonds I, Yao Y and Zhong L 2023a Bidimensional climatology and trends of Northern Hemisphere blocking utilizing a new detection method *Q. J. R. Meteorol. Soc.* **149** 1932–52

Li Q, Zhang S, Huang K, Huang C, Gong Y, Tang W and Ma Z 2024 Long-term variation of Arctic sudden stratospheric warmings (SSW) and potential causes *Earth Planet. Phys.* **8** 742–52

Li X, Zhang Y-J and Gao H 2022 The extreme cold wave in early November 2021 in China and the influences from the meridional pressure gradient over East Asia *Adv. Clim. Change Res.* **13** 797–802

Li Y, Kirchengast G, Schwaerz M and Yuan Y 2023b Monitoring sudden stratospheric warmings under climate change since 1980 based on reanalysis data verified by radio occultation *Atmos. Chem. Phys.* **23** 1259–84

Liang Z, Rao J, Guo D, Lu Q and Shi C 2023 Northern winter stratospheric polar vortex regimes and their possible influence on the extratropical tropopause *Clim. Dyn.* **60** 3167–86

Lin H 2009 Global extratropical response to diabatic heating variability of the Asian summer monsoon *J. Atmos. Sci.* **66** 2697–713

Lin H, Yu B and Hall N M J 2022 Origin of the warm Arctic–cold North American pattern on the intraseasonal time scale *J. Atmos. Sci.* **79** 2571–258

Lin L, Wang Z, Xu Y and Fu Q 2016 Sensitivity of precipitation extremes to radiative forcing of greenhouse gases and aerosols *Geophys. Res. Lett.* **43** 9860–8

Lu H, Bracegirdle T J, Phillips T, Bushell A and Gray L 2014 Mechanisms for the Holtan-Tan relationship and its decadal variation *J. Geophys. Res.* **119** 2811–30

Lu Q, Rao J, Shi C, Ren R, Liu Y and Liu S 2023 Stratosphere-troposphere coupling during stratospheric extremes in the 2022/23 winter *Weather Clim. Extrem.* **42** 100627

Luo B *et al* 2024 Rapid summer Russian Arctic sea-ice loss enhances the risk of recent Eastern Siberian wildfires *Nat. Commun.* **15** 5399

Luo B, Luo D, Dai A, Simmonds I and Wu L 2021 A connection of winter Eurasian cold anomaly to the modulation of Ural blocking by ENSO *Geophys. Res. Lett.* **48** e2021GL094304

Luo B, Luo D, Dai A, Simmonds I and Wu L 2022 The modulation of Interdecadal Pacific Oscillation and Atlantic Multidecadal Oscillation on winter Eurasian cold anomaly via the Ural blocking change *Clim. Dyn.* **59** 127–50

Luo B, Luo D, Wu L, Zhong L and Simmonds I 2017 Atmospheric circulation patterns which promote winter Arctic sea ice decline *Environ. Res. Lett.* **12** 054017

Luo D 1991 Nonlinear Schrodinger equation in the rotating barotropic atmosphere and atmospheric blocking *J. Meteorol. Res.* **5** 587–97

Luo D 2000 Planetary-scale envelope Rossby solitons in a two-layer model and their interaction with synoptic-scale eddies *Dyn. Atmos. Oceans* **32** 27–74

Luo D, Chen X, Overland J, Simmonds I, Wu Y and Zhang P 2019b Weakened potential vorticity barrier linked to recent winter Arctic sea ice loss and midlatitude cold extremes *J. Clim.* **32** 4235–61

Luo D, Luo B and Zhang W 2023 A perspective on the evolution of atmospheric blocking theories: from eddy-mean flow interaction to nonlinear multiscale interaction *Adv. Atmos. Sci.* **40** 553–6

Luo D, Xiao Y, Yao Y, Dai A, Simmonds I and Franzke C 2016 The impact of Ural blocking on winter warm Arctic-cold Eurasian anomalies. Part I: blocking-induced amplification *J. Clim.* **29** 3925–47

Luo D and Zhang W 2020 A nonlinear multi-scale theory of atmospheric blocking: dynamical and thermodynamic effects of meridional potential vorticity gradient *J. Atmos. Sci.* **77** 2471–550

Luo D, Zhang W, Zhong L and Dai A 2019a A nonlinear theory of atmospheric blocking: a potential vorticity gradient view *J. Atmos. Sci.* **76** 2399–427

Ma J, Chen W, Nath D and Lan X 2020 Modulation by ENSO of the relationship between stratospheric sudden warming and the Madden–Julian Oscillation *Geophys. Res. Lett.* **47** e2020GL088894

Ma T, Chen W, An X, Garfinkel C I and Cai Q 2023 Nonlinear effects of the stratospheric Quasi–Biennial Oscillation and ENSO on the North Atlantic winter atmospheric circulation *J. Geophys. Res. Atmos.* **128** e2023JD039537

Ma W *et al* 2024 The role of interdecadal climate oscillations in driving Arctic atmospheric river trends *Nat. Commun.* **15** 2135

Ma W, Chen G, Peings Y and Alviz N 2021 Atmospheric river response to Arctic sea ice loss in the Polar Amplification Model Intercomparison Project *Geophys. Res. Lett.* **48** e2021GL094883

Ma X, Wang L, Smith D, Hermanson L, Eade R, Dunstone N, Hardiman S and Zhang J 2022 ENSO and QBO modulation of the relationship between Arctic sea ice loss and Eurasian winter climate *Environ. Res. Lett* **17** 124016

Matthias V and Kretschmer M 2020 The influence of stratospheric wave reflection on North American cold spell *Mon. Weather Rev.* **148** 1675–90

McCusker K E, Fyfe J C and Sigmond M 2016 Twenty-five winters of unexpected Eurasian cooling unlikely due to Arctic sea-ice loss *Nat. Geosci.* **9** 838–43

Messori G, Kretschmer M, Lee S H and Wendt V 2022 Stratospheric downward wave reflection events modulate North American weather regimes and cold spells *Weather Clim. Dyn.* **3** 1215–36

Moon W, Kim B-M, Yang G-H and Wettlaufer J S 2022 Wavier jet streams driven by zonally asymmetric surface thermal forcing *Proc. Natl Acad. Sci.* **119** e2200890119

Mori M, Watanabe M, Shiogama H, Inoue J and Kimoto M 2014 Robust Arctic sea-ice influence on the frequent Eurasian cold winters in past decades *Nat. Geosci.* **7** 869–73

Na Y, Fu Q and Kodama C 2020 Precipitation probability and its future changes from a global cloud-resolving model and CMIP6 simulations *J. Geophys. Res. Atmos.* **125** e2019JD031926

Nakamura T, Yamazaki K, Iwamoto K, Honda M, Miyoshi Y, Ogawa Y, Tomikawa Y and Ukita J 2016 The stratospheric pathway for Arctic impacts on midlatitude climate *Geophys. Res. Lett.* **43** 3494–501

Nakamura T, Yamazaki K, Iwamoto K, Honda M, Miyoshi Y, Ogawa Y and Ukita J 2015 A negative phase shift of the winter AO/NAO due to the recent Arctic sea-ice reduction in late autumn *J. Geophys. Res. Atmos.* **120** 3209–27

NOAA National Centers for Environmental Information (NCEI) 2023 *U.S. Billion-Dollar Weather and Climate Disasters* (available at: www.climate.gov/news-features/blogs/2022-us-billion-dollar-weather-and-climate-disasters-historical-context and www.climate.gov/news-features/blogs/beyond-data/2021-us-billion-dollar-weather-and-climate-disasters-historical)

Nygård T, Papritz L, Naakka T and Vihma T 2023 Cold wintertime air masses over Europe: where do they come from and how do they form? *Weather Clim. Dyn.* **4** 943–61

Outten S *et al* 2023 Reconciling conflicting evidence for the cause of the observed early 21st century Eurasian cooling *Weather Clim. Dyn.* **4** 95–114

Outten S and Esau I 2012 A link between Arctic sea ice and recent cooling trends over Eurasia *Clim. Change* **110** 1069–75

Overland J E 2016 A difficult Arctic science issue: midlatitude weather linkages *Polar Sci.* **10** 210–6

Overland J E *et al* 2021 How do intermittency and simultaneous processes obfuscate the Arctic influence on midlatitude winter extreme weather events? *Environ. Res. Lett* **16** 043002

Overland J E 2024 Emergence of Arctic extremes *Climate* **12** 109

Overland J E, Francis J A, Hall R, Hanna E, Kim S-J and Vihma T 2015 The melting Arctic and midlatitude weather patterns: are they connected? *J. Clim.* **28** 7917–32

Overland J, Dethloff K, Francis J A, Hall R J, Hanna E, Kim S-J, Screen J A, Shepherd T G and Vihma T 2016 Nonlinear response of midlatitude weather to the changing Arctic *Nat. Clim. Change* **6** 992–8

Overland J, Wood K R and Wang M 2011 Warm Arctic-cold continents: climate impacts of the newly open arctic sea *Polar. Res.* **30** 15787

Pahlavan H A, Fu Q, Wallace J M and Kiladis G N 2021a Revisiting the Quasi–Biennial Oscillation as seen in ERA5. Part I: description and momentum budget *J. Atmos. Sci.* **78** 673–91

Pahlavan H A, Wallace J M, Fu Q and Kiladis G N 2021b Revisiting the Quasi–Biennial Oscillation as seen in ERA5. Part II: evaluation of waves and wave forcing *J. Atmos. Sci.* **78** 693–707

Peings Y 2019 Ural blocking as a driver of early-winter stratospheric warmings *Geophys. Res. Lett.* **46** 5460–8

Peings Y, Cattiaux J and Magnusdottir G 2019 The polar stratosphere as an arbiter of the projected tropical versus polar tug of war *Geophys. Res. Lett.* **46** 9261–70

Peings Y, Davini P and Magnusdottir G 2023 Impact of Ural blocking on early winter climate variability under different Barents–Kara sea ice conditions *J. Geophys. Res. Atmos.* **128** e2022JD036994

Peings Y, Labe Z M and Magnusdottir G 2021 Are 100 ensemble members enough to capture the remote atmospheric response to $+2\,°C$ Arctic sea ice loss? *J. Clim.* **34** 3751–69

Pithan F and Mauritsen T 2014 Arctic amplification dominated by temperature feedbacks in contemporary climate models *Nat. Geosci.* **7** 181–4

Polyakov I V, Ingvaldsen R B, Pnyushkov A V, Bhatt U S, Francis J A, Janout M, Kwok R and Skagseth O 2023 Fluctuating Atlantic inflows modulate Arctic atlantification *Science* **381** 972–9

Previdi M, Smith K L and Polvani L M 2021 Arctic amplification of climate change: a review of underlying mechanisms *Environ. Res. Lett.* **16** 093003

Qi Y, Yu H, Fu Q, Chen Q, Ran J and Yang Z 2022 Future changes in drought frequency due to changes in the mean and shape of the PDSI probability density function under RCP4.5 scenario *Front. Earth Sci.* **10** 857885

Qian Q, Wu K, Leung J C-H and Shi J 2016b Long-term trends of the polar and Arctic cells influencing the Arctic climate since 1989 *J. Geophys. Res. Atmos.* **121** 2679–90

Qian W, Wu K and Liang H 2016a Arctic and Antarctic cells in the troposphere *Theor. Appl. Climatol.* **125** 1–12

Rantanen M, Hyvärinen O, Vajda A and Karpechko A 2024 The atmospheric 'cold blob' over Fennoscandia from October 2023 to January 2024 *Weather* (https://doi.org/10.1002/wea.4570)

Rantanen M, Karpechko A Y, Lipponen A, Nordling K, Hyvärinen O, Ruosteenoja K, Vihma T and Laaksonen A 2022 The Arctic has warmed nearly four times faster than the globe since 1979 *Commun. Earth Environ.* **3** 168

Rogers C D W, Kornhuber K, Perkins-Kirkpatrick S E, Loikith P C and Singh D 2022 Sixfold increase in historical northern hemisphere concurrent large heatwaves driven by warming and changing atmospheric circulations *J. Clim.* **35** 1063–78

Samarasinghe S M, McGraw M C, Barnes E A and Ebert-Uphoff I 2019 A study of links between the Arctic and the midlatitude jet stream using Granger and Pearl causality *Environmetrics* **30** e2540

Schulzweida U 2019 CDO user guide *Zenodo* (https://doi.org/10.5281/zenodo.3539275)

Screen J A 2014 Arctic amplification decreases temperature variance in northern mid- to high-latitudes *Nat. Clim. Change* **4** 577–82

Screen J A and Blackport R 2019 Is sea-ice-driven Eurasian cooling too weak in models *Nat. Clim. Change* **9** 934–6

Screen J, Deser C and Sun L 2015 Projected changes in regional climate extremes arising from Arctic sea ice loss *Environ. Res. Lett.* **10** 084006

Seneviratne S I *et al* 2021 Weather and climate extreme events in a changing climate *Climate Change 2021: The Physical Science Basis. Contribution of Working Group I to the Sixth Assessment Report of the Intergovernmental Panel on Climate Change* ed V Masson-Delmotte *et al* (Cambridge University Press) pp 1513–766

Seo K H and Son S 2012 The global atmospheric circulation response to tropical diabatic heating associated with the Madden—Julian Oscillation during Northern Winter *J. Atmos. Sci.* **69** 79–96

Shaw T A, Perlwitz J and Weiner O 2014 Troposphere-stratosphere coupling: links to North Atlantic weather and climate, including their representation in CMIP5 models *J. Geophys. Res. Atmos.* **119** 5864–80

Shen X, Wang L, Scaife A A, Hardiman S C and Xu P 2023 The Stratosphere–Troposphere Oscillation as the dominant intraseasonal coupling mode between the stratosphere and troposphere *J. Clim.* **36** 2259–76

Shepherd T 2021 Bringing physical reasoning into statistical practice in climate change science *Clim. Change* **169** 2

Siew P Y F, Li C, Sobolowski S P and King M P 2020 Intermittency of Arctic–midlatitude teleconnections: stratospheric pathway between autumn sea ice and the winter North Atlantic Oscillation *Weather Clim. Dyn.* **1** 261–75

Singh D, Bekris Y S, Rogers C D W, Doss-Gollin J, Coffel E D and Kalashnikov D A 2024 Enhanced solar and wind potential during widespread temperature extremes across the U.S. interconnected energy grids *Environ. Res. Lett.* **19** 044018

Smith A, Smith D, Cohen J and Jones M 2021 Arctic warming amplifies climate change and its impacts *ScienceBrief* pp 1–4

Smith D M *et al* 2019 The Polar Amplification Model Intercomparison Project (PAMIP) contribution to CMIP6: investigating the causes and consequences of polar amplification *Geosci. Model Dev.* **12** 1139–64

Smith D M *et al* 2022 Robust but weak winter atmospheric circulation response to future Arctic sea ice loss *Nat. Commun.* **13** 727

Smith E T and Sheridan S C 2019 The influence of atmospheric circulation patterns on cold air outbreaks in the eastern United States *Int. J. Climatol.* **39** 2080–95

Song Y Y, Yao Y, Luo D H and Li Y L 2023 Loss of autumn Kara–East Siberian Sea ice intensifies winter Ural blocking and cold anomalies in high latitudes of Eurasia *Atmos. Res.* **295** 107038

Statnaia I A, Karpechko A Y and Järvinen H J 2020 Mechanisms and predictability of sudden stratospheric warming in winter 2018 *Weather Clim. Dyn.* **1** 657–74

Statnaia I, Karpechko A Y, Kämäräinen M and Järvinen H 2022 Stratosphere–troposphere coupling enhances subseasonal predictability of Northern Eurasian cold spells *Q. J. R. Meteorol. Soc.* **148** 2769–83

Sterk H A M, Steeneveld G J, Bosveld F, Vihma T, Anderson P S and Holtslag A A M 2016 Clear-sky stable boundary layers with low winds over snow-covered surfaces. Part 2: process sensitivity *Q. J. R. Meteorol. Soc.* **142** 821–35

Sui C, Yu L and Vihma T 2020 Occurrence and drivers of wintertime temperature extremes in Northern Europe during 1979–2016 *Tellus* A **72** 1–19

Sun L, Deser C, Simpson I and Sigmond M 2022 Uncertainty in the winter tropospheric response to Arctic sea ice loss: the role of stratospheric polar vortex internal variability *J. Clim.* **35** 3109–30

Sun L, Perlwitz J and Hoerling M 2016 What caused the recent 'Warm Arctic, Cold Continents' trend pattern in winter temperatures? *Geophys. Res. Lett.* **43** 5345–52

Sweeney A J, Fu Q, Po-Chedley S, Wang H and Wang M 2023 Internal variability increased Arctic amplification during 1980–2022 *Geophys. Res. Lett.* **50** e2023GL106060

Sweeney A J, Fu Q, Po-Chedley S, Wang H and Wang M 2024 Unique temperature trend pattern associated with internally driven global cooling and Arctic warming during 1980–2022 *Geophys. Res. Lett.* **51** e2024GL108798

Tachibana Y, Komatsu K K, Alexeev V A, Cai L and Ando Y 2019 Warm hole in Pacific Arctic sea ice cover forced mid-latitude Northern Hemisphere cooling during winter 2017–18 *Sci. Rep.* **9** 5567

Takaya K and Nakamura H 2005 Geographical dependence of upper-level blocking formation associated with intraseasonal amplification of the Siberian High *J. Clim.* **62** 4441–9

Tan X and Bao M 2020 Linkage between a dominant mode in the lower stratosphere and the Western Hemisphere circulation pattern *Geophys. Res. Lett.* **47** e2020GL090105

Taylor P C *et al* 2022 Process drivers, inter-model spread, and the path forward: a review of amplified Arctic warming *Front. Earth Sci.* **9** 758361

Thompson D W J, Baldwin M P and Wallace J M 2002 Stratospheric connection to Northern Hemisphere wintertime weather: implications for prediction *J. Clim.* **15** 1421–8

Tyrlis E, Bader J, Manzini E, Ukita J, Nakamura H and Matei D 2020 On the role of Ural blocking in driving the warm Arctic-cold Siberian pattern *Q. J. R. Meteorol. Soc.* **146** 2138–53

Tyrlis E, Manzini E, Bader J, Ukita J, Nakamura H and Matei D 2017 Ural blocking driving extreme Arctic sea ice loss, Cold Eurasia and stratospheric vortex weakening in autumn and early winter 2016–17 *J. Geophys. Res. Atmos.* **124** 11313–29

Vihma T *et al* 2020 Effects of the tropospheric large-scale circulation on European winter temperatures during the period of amplified Arctic warming *Int. J. Climatol.* **40** 509–29

Wallace J M, Fu Q, Smoliak B V, Lin P and Johanson C M 2012 Simulated versus observed patterns of warming over the extratropical Northern Hemisphere continents during the cold season *Proc. Natl Acad. Sci. USA* **109** 14337–42

Walsh A, Screen J A, Scaife A A and Smith D M 2022 Non-linear response of the extratropics to tropical climate variability *Geophys. Res. Lett.* **49** e2022GL100416

Wang H and Luo D 2022 North Atlantic footprint of summer Greenland ice sheet melting on interannual to interdecadal time scales: a Greenland blocking perspective *J. Clim.* **35** 1939–61

Waznah H, Gachon P, Laprise R, de Vernal A and Tremblay B 2021 Atmospheric blocking events in the North Atlantic trends and links to climate anomalies and teleconnections *Clim. Dyn.* **56** 2199–221

Wegmann M *et al* 2015 Arctic moisture source for Eurasian snow cover variations in autumn *Environ. Res. Lett.* **10** 054015

Weinberger I, Garfinkel C I, Harnik N and Paldor N 2022 Transmission and reflection of upward propagating Rossby waves in the lowermost stratosphere: importance of the tropopause inversion layer *J. Atmos. Sci.* **79** 3263–74

Wendisch M *et al* 2023 Atmospheric and surface processes and feedback mechanisms determining Arctic amplification: a review of first results and prospects of the (AC)³ project *Bull. Am. Meteorol. Soc.* **104** E208–42

White C J *et al* 2021 Advances in the application and utility of subseasonal-to-seasonal predictions *Bull. Am. Meteorol. Soc.* **57** E1448–72

White I, Garfinkel C I, Gerber E P, Jucker M, Aquila V and Oman L D 2019 The downward influence of sudden stratospheric warmings: association with tropospheric precursors *J. Clim.* **32** 85–108

Wickström S, Jonassen M, Vihma T and Uotila P 2020 Trends in cyclones in the high latitude North Atlantic during 1979–2016 *Q. J. R. Meteorol. Soc.* **146** 762–79

Woollings T, Barriopedro D, Methven J, Son S-W, Martius O, Harvey B, Sillmann J, Lupo A R and Seneviratne S 2018 Blocking and its response to climate change *Curr. Clim. Change Rep.* **4** 287–300

Xu X, He S, Gao Y, Zhou B and Wang H 2021 Contributors to linkage between Arctic warming and East Asian winter climate *Clim. Dyn.* **57** 2543–55

Yamazaki K, Nakamura T, Ukita J and Hoshi K 2020 A tropospheric pathway of the stratospheric oscillation (QBO) impact on the boreal winter polar vortex *Atmos. Chem. Phys.* **20** 5111–27

Yao Y *et al* 2023 Extreme cold events in North America and Eurasia in November–December 2022: a potential vorticity gradient perspective *Adv. Atmos. Sci.* **40** 953–62

Yao Y, Luo D H, Dai A G and Feldstein S B 2016 The Positive North Atlantic Oscillation with downstream blocking and Middle East snowstorms: impacts of the North Atlantic Jet *J. Clim.* **29** 1853–76

Yao Y, Zhang W Q, Luo D H, Zhong L H and Pei L 2022 Seasonal cumulative effect of Ural blocking episodes on the frequent cold events in China during the early winter of 2020/21 *Adv. Atmos. Sci.* **39** 609–24

Ye K and Jung T 2019 How strong is influence of the tropics and midlatitudes on the Arctic atmospheric circulation and climate change? *Geophys. Res. Lett.* **46** 4942–52

Ye K, Jung T and Semmler T 2018 The influences of the Arctic troposphere on the midlatitude climate variability and the recent Eurasian cooling *J. Geophys. Res. Atmos.* **123** 10162–84

Ye K and Messori G 2020 Two leading modes of wintertime atmospheric circulation drive the recent warm Arctic-cold Eurasia temperature pattern *J. Clim.* **33** 5565–87

Ye K and Messori G 2021 Inter-model spread in the wintertime Arctic amplification in the CMIP6 models and the important role of internal climate variability *Glob. Planet. Change* **204** 103543

Ye K, Woollings T and Screen J A 2023 European winter climate response to projected Arctic Sea-ice loss strongly shaped by change in the North Atlantic Jet *Geophys. Res. Lett.* **50** e2022GL102005

Ye K, Woollings T and Sparrow S N 2024b Dynamic and thermodynamic control of the response of winter climate and extreme weather to projected Arctic sea-ice loss *Geophys. Res. Lett.* **51** e2024GL109271

Ye K, Woollings T, Sparrow S, Watson P and Screen J 2024a Response of winter climate and extreme weather to projected Arctic sea-ice loss in very large-ensemble climate model simulations *npj Clim. Atmos. Sci.* **7** 20

Zhang C 2005 Madden–Julian oscillation *Rev. Geophys.* **43** RG2003

Zhang P, Wu Y, Chen G and Yu Y 2020 North American cold events following sudden stratospheric warming in the presence of low Barents–Kara Sea sea ice *Environ. Res. Lett* **15** 124017

Zhang P, Wu Y, Simpson I, Smith K, Zhang X, De B and Callaghan P 2018a A stratospheric pathway linking a colder Siberia to Barents–Kara sea ice loss *Sci. Adv.* **4** eaat6025

Zhang R, Screen J A and Zhang R 2022a Arctic and Pacific Ocean conditions were favourable for cold extremes over Eurasia and North America during winter 2020/21 *Bull. Am. Meteorol. Soc.* **103** E2285–301

Zhang R, Wang H, Fu Q, Pendergrass A G, Wang M, Yang Y, Ma P-L and Rasch P J 2018b Local radiative feedbacks over the Arctic based on observed short-term climate variations *Geophys. Res. Lett.* **45** 5761–70

Zhang W and Luo D 2020 A nonlinear theory of atmospheric blocking: an application to Greenland blocking changes linked to winter Arctic sea ice loss *J. Atmos. Sci.* **77** 723–51

Zhang X, Fu Y, Han Z, Overland J E, Rinke A, Tang H, Vihma T and Wang M 2022b Extreme cold events from East Asia to North America in winter 2020/21: comparisons, causes, and future implications *Adv. Atmos. Sci.* **39** 553–65

Zhang Y, Yi Y, Ren X and Liu Y 2021 Statistical characteristics and long-term variations of major sudden stratospheric warming events *J. Meteorol. Res.* **35** 416–27

Zheng F *et al* 2021 The 2020/21 extremely cold winter in China influenced by the synergistic effect of La Niña and warm Arctic *Adv. Atmos. Sci.* **39** 546–52

Zhou W, Leung L R and Lu J 2024 Steady threefold Arctic amplification of externally forced warming masked by natural variability *Nat. Geosci.* **17** 508–15

Zhuo W Q, Yao Y, Luo D H, Simmonds I and Huang F 2022 Combined impact of the cold vortex and atmospheric blocking on cold outbreaks over East Asia and the potential for short-range prediction of such occurrences *Environ. Res. Lett.* **17** 084037

Zou Y, Rasch P J, Wang H, Xie Z and Zhang R 2021 Increasing large wildfires over the western United States linked to diminishing sea ice in the Arctic *Nat. Commun.* **12** 6048